



Database:	US Patents Full-Text Database US Pre-Grant Publication Full-Text Database JPO Abstracts Database EPO Abstracts Database Derwent World Patents Index IBM Technical Disclosure Bulletins						
Term:	L21 and ((continuous\$3 or constant\$4 or "without stopping" or convey\$5) with (move or moving or moved or motion or movement))						
Display: Generate:	Documents in Display Format: - Starting with Number 1 O Hit List • Hit Count O Side by Side O Image						
Search Clear Help Logout Interrupt							
Main Menu Show S Numbers Edit S Numbers Preferences Cases							
Search History							

DATE: Wednesday, January 29, 2003 Printable Copy Create Case

Set Name side by side	Query	Hit Count	Set Name result set
DB=US	PT,PGPB,JPAB,EPAB,DWPI,TDBD; PLUR=YES; OP=ADJ		
1 77	L21 and ((continuous\$3 or constant\$4 or "without stopping" or convey\$5) with (move or moving or moved or motion or movement))	14	<u>L22</u>
<u>L21</u>	L19 and ((move or moving or moved or motion or movement) with (bolus or contrast or table or gantry or stretcher or bed or support or platform or object or subject or patient))	29	<u>L21</u>
<u>L20</u>	L19 and ((move or moving or moved or motion or movement) with (bolus or contrast or table or gantry or stretcher or bed or support or platform))	14	<u>L20</u>
119	L18 and (bolus or contrast or table or gantry or stretcher or bed or support or platform)	56	<u>L19</u>
<u>L18</u>	L17 and (move or moving or moved or motion or movement)	59	<u>L18</u>
<u>L17</u>	L11 and ((field with view) or FOV)	60	<u>L17</u>
<u>L16</u>	L14 and (field with view)	9	<u>L16</u>
117	L13 and (bolus or contrast or table or gantry or stretcher or bed or support or platform)	12	<u>L15</u>
1 14	L12 and (bolus or contrast or table or gantry or stretcher or bed or support or platform)	13	<u>L14</u>
<u>L13</u>	L12 and (move or moving or moved or motion or movement)	15	<u>L13</u>
11/	L11 and ((slab or (volume with slice)) with (thick or thickness or depth))	16	<u>L12</u>
1 1 1	L10 and (read or readout or read-out or frequency or acquir\$4 or acquisition or aq)	81	<u>L11</u>
<u>L10</u>	L9 and (excit\$5 or encod\$5)	81	<u>L10</u>
<u>L9</u>	L8 and (filter\$4)	104	<u>L9</u>
<u>L8</u>	L7 and (thick or thickness or depth)	183	<u>L8</u>
<u>L7</u>	L6 and (direction)	278	<u>L7</u>
<u>L6</u>	L5 and ((continuous\$3 or constant\$4 or "without stopping" or convey\$5) with ((imaging or image or imaged) with (volume or region or area or zone or object or subject or patient)))	316	<u>L6</u>
1 1	L4 and (FOV or "field of view" or field-of-view or ROI or voi or ((volume or region or area or zone) with (interest or investigation)))	1937	<u>L5</u>
<u>L4</u>	L3 and (track\$4 or follow\$4 or map\$5)	4494	<u>L4</u>
1 1	L2 and ((imaging or image or imaged) with (volume or region or area or zone or object or subject or patient))	4961	<u>L3</u>
1 /	L1 and (slab or boundary or artifact or venetian or blind or SBA or VB or VBA or (volume with slice))	12997	<u>L2</u>
<u>L1</u>	((magnetic adj resonance) or MRI or NMR)	140481	<u>L1</u>

END OF SEARCH HISTORY

Generate Collection

Print

Search Results - Record(s) 1 through 13 of 13 returned.

1. Document ID: US 20030011369 A1

L14: Entry 1 of 13

File: PGPB

Jan 16, 2003

PGPUB-DOCUMENT-NUMBER: 20030011369

PGPUB-FILING-TYPE: new

DOCUMENT-IDENTIFIER: US 20030011369 A1

TITLE: Moving table MRI with frequency-encoding in the z-direction

PUBLICATION-DATE: January 16, 2003

INVENTOR - INFORMATION:

NAME

CITY

STATE

COUNTRY

RULE-47

Brittain, Jean H.

Palo Alto

CA

US

Pauly, John M.

Redwood City

CA

US

US-CL-CURRENT: 324/309; 324/307, 324/318

Full Title Citation Front Review Classification Date Reference Sequences Attachments Claims KMC Draw Desc Image

2. Document ID: US 20030006770 A1

L14: Entry 2 of 13

File: PGPB

Jan 9, 2003

PGPUB-DOCUMENT-NUMBER: 20030006770

PGPUB-FILING-TYPE: new

DOCUMENT-IDENTIFIER: US 20030006770 A1

TITLE: Quantitation and standardization of magnetic resonance measurements

PUBLICATION-DATE: January 9, 2003

INVENTOR - INFORMATION:

NAME

1 of 6

CITY

STATE

COUNTRY

RULE-47

Smith, Justin P.

Kirkland

WA

US

US-CL-CURRENT: 324/309; 324/300, 324/314, 324/318

Full Title Citation Front Review Classification Date Reference Sequences Attachments Claims KMC Draw, Desc Image

3. Document ID: US 20020140423 A1

L14: Entry 3 of 13

File: PGPB

Oct 3, 2002

PGPUB-DOCUMENT-NUMBER: 20020140423

PGPUB-FILING-TYPE: new

DOCUMENT-IDENTIFIER: US 20020140423 A1

TITLE: Moving table MP with frequency-encoding in the Direction

PUBLICATION-DATE: October 3, 2002

INVENTOR-INFORMATION:

NAME CITY STATE COUNTRY RULE-47

Brittain, Jean Helen Menlo Park CA US

US-CL-CURRENT: 324/301; 324/309

Full Title Citation Front Review Classification Date Reference Sequences Attachments

Draw Desc Image

4. Document ID: US 20020103429 A1

L14: Entry 4 of 13 File: PGPB Aug 1, 2002

PGPUB-DOCUMENT-NUMBER: 20020103429

PGPUB-FILING-TYPE: new

DOCUMENT-IDENTIFIER: US 20020103429 A1

TITLE: Methods for physiological monitoring, training, exercise and regulation

PUBLICATION-DATE: August 1, 2002

INVENTOR-INFORMATION:

NAME CITY STATE COUNTRY RULE-47

deCharms, R. Christopher Moss Beach CA US

US-CL-CURRENT: 600/410

Full Title Citation Front Review Classification Date Reference Sequences Attachments KWC |
Draws Description

5. Document ID: US 20020103428 A1

L14: Entry 5 of 13 File: PGPB Aug 1, 2002

PGPUB-DOCUMENT-NUMBER: 20020103428

PGPUB-FILING-TYPE: new

DOCUMENT-IDENTIFIER: US 20020103428 A1

TITLE: Methods for physiological monitoring, training, exercise and regulation

PUBLICATION-DATE: August 1, 2002

INVENTOR-INFORMATION:

NAME CITY STATE COUNTRY RULE-47

deCharms, R. Christopher Moss Beach CA US

US-CL-CURRENT: 600/410

Full Title Citation Front Review Classification Date Reference Sequences Attachments KMC Draw Desc Image

6. Document ID: US 6396270 B1

L14: Entry 6 of 13 File: USPT May 28, 2002

US-PAT-NO: 6396270

DOCUMENT-IDENTIFIER: US 6396270 B1

TITLE: Quantitation and standardization of magnetic resonance measurements

DATE-ISSUED: May 28, 2002

INVENTOR-INFORMATION:

NAME

CITY

STATE

ZIP CODE

COUNTRY

Smith; Justin P.

Kirkland

WA

US-CL-CURRENT: 324/309; 324/307

Full Title Citation Front Review Classification Date Reference Sequences Attachments KMC |

7. Document ID: US 5928148 A

L14: Entry 7 of 13

File: USPT

Jul 27, 1999

US-PAT-NO: 5928148

DOCUMENT-IDENTIFIER: US 5928148 A

TITLE: Method for performing magnetic resonance angiography over a large field of

view using table stepping

DATE-ISSUED: July 27, 1999

INVENTOR-INFORMATION:

NAME

CITY

STATE

ZIP CODE

COUNTRY

Wang; Yi

New York

New York

NY NY

Lee; Howard M. Khilnani; Neil M. Rye

NY

US-CL-CURRENT: 600/420; 324/306, 600/415

Full Title Citation Front Review Classification Date Reference Sequences Attachments

8. Document ID: US 5818231 A

L14: Entry 8 of 13

File: USPT

Oct 6, 1998

Keac

US-PAT-NO: 5818231

DOCUMENT-IDENTIFIER: US 5818231 A

TITLE: Quantitation and standardization of magnetic resonance measurements

DATE-ISSUED: October 6, 1998

INVENTOR-INFORMATION:

NAME

CITY

STATE

ZIP CODE

COUNTRY

Smith; Justin P.

Kirkland

WA

US-CL-CURRENT: 324/309; 324/307

9. Document ID: US 5685305 A

L14: Entry 9 of 13

File: USPT

Nov 11, 1997

US-PAT-NO: 5685305

DOCUMENT-IDENTIFIER: US 5685305 A

TITLE: Method and system for MRI detection of abnormal blood flow

DATE-ISSUED: November 11, 1997

INVENTOR - INFORMATION:

NAME

CITY

STATE

ZIP CODE

COUNTRY

Moonen; Chrit T. W.

Kensington Kensington MD MD

van Gelderen; Peter

Duyn; Jeff

Kensington

MD

US-CL-CURRENT: 600/419; 324/306

Full Title Citation Front Review Classification Date Reference Sequences Attachments

Draws Desc Image

KWIC

10. Document ID: US 5644232 A

L14: Entry 10 of 13

File: USPT

Jul 1, 1997

US-PAT-NO: 5644232

DOCUMENT-IDENTIFIER: US 5644232 A

TITLE: Quantitation and standardization of magnetic resonance measurements

DATE-ISSUED: July 1, 1997

INVENTOR-INFORMATION:

NAME

CITY

STATE

ZIP CODE

COUNTRY

Smith; Justin P.

Kirkland

WA

US-CL-CURRENT: 324/304; 324/308

Full | Title | Citation | Front | Review | Classification | Date | Reference | Sequences | Attachments |
Draws Desc | Image |

KWIC

11. Document ID: US 5544652 A

L14: Entry 11 of 13

File: USPT

Aug 13, 1996

US-PAT-NO: 5544652

DOCUMENT-IDENTIFIER: US 5544652 A

TITLE: Ultrafast burst imaging using shifting of excited regions

DATE-ISSUED: August 13, 1996

INVENTOR-INFORMATION:

NAME

CITY

STATE

ZIODE

COUNTRY

Duyn; Jozef H.

Kensington

MD

ODE CO

US-CL-CURRENT: 600/410; 324/309

Full Title Citation Front Review Classification Date Reference Sequences Attachments

Draw, Desc Image

12. Document ID: US 5361763 A

L14: Entry 12 of 13

File: USPT

Nov 8, 1994

US-PAT-NO: 5361763

DOCUMENT-IDENTIFIER: US 5361763 A

TITLE: Method for segmenting features in an image

DATE-ISSUED: November 8, 1994

INVENTOR - INFORMATION:

NAME

CITY

Y STATE

ZIP CODE

COUNTRY

Kao; Yi-Hsuan
Sorenson; James A.

Madison Madison WI

Bahn; Mark M.

Madison

WI

US-CL-CURRENT: 600/410; 382/145, 382/174

Full Title Citation Front Review Classification Date Reference Sequences Attachments

Draw, Desc Image

13. Document ID: US 4431968 A

L14: Entry 13 of 13

File: USPT

Feb 14, 1984

KWIC

US-PAT-NO: 4431968

DOCUMENT-IDENTIFIER: US 4431968 A

TITLE: Method of three-dimensional NMR imaging using selective excitation

DATE-ISSUED: February 14, 1984

INVENTOR-INFORMATION:

NAME

CITY

STATE

ZIP CODE

COUNTRY

KWIC

Edelstein; William A.

Schenectady

NY

Bottomley; Paul A.

Clifton Park

NY

US-CL-CURRENT: 324/309; 324/311

Full Title Citation Front Review Classification Date Reference Sequences Attachments

Draws Descriptings

Print

Generate Collection

Term	Documents
BOLUS.DWPI,TDBD,EPAB,JPAB,USPT,PGPB.	15023
BOLU.DWPI,TDBD,EPAB,JPAB,USPT,PGPB.	2
CONTRAST.DWPI,TDBD,EPAB,JPAB,USPT,PGPB.	510735
CONTRASTS.DWPI,TDBD,EPAB,JPAB,USPT,PGPB.	14345
TABLE.DWPI,TDBD,EPAB,JPAB,USPT,PGPB.	1148868
TABLES.DWPI,TDBD,EPAB,JPAB,USPT,PGPB.	216755
GANTRY.DWPI,TDBD,EPAB,JPAB,USPT,PGPB.	12614
GANTRIES.DWPI,TDBD,EPAB,JPAB,USPT,PGPB.	797
GANTRYS.DWPI,TDBD,EPAB,JPAB,USPT,PGPB.	19
STRETCHER.DWPI,TDBD,EPAB,JPAB,USPT,PGPB.	9652
STRETCHERS.DWPI,TDBD,EPAB,JPAB,USPT,PGPB.	2230
(L12 AND (BOLUS OR CONTRAST OR TABLE OR GANTRY OR STRETCHER OR BED OR SUPPORT OR PLATFORM)).USPT,PGPB,JPAB,EPAB,DWPI,TDBD.	13

There are more results than shown above. Click here to view the entire set.

Display Format:	Change Format
-----------------	---------------

Previous Page Next Page

Generate Collection

Print

Search Results - Record(s) 1 through 14 of 14 returned.

1. Document ID: US 20030011369 A1

L22: Entry 1 of 14

File: PGPB

Jan 16, 2003

PGPUB-DOCUMENT-NUMBER: 20030011369

PGPUB-FILING-TYPE: new

DOCUMENT-IDENTIFIER: US 20030011369 A1

TITLE: Moving table MRI with frequency-encoding in the z-direction

PUBLICATION-DATE: January 16, 2003

INVENTOR-INFORMATION:

NAME

CITY

STATE

COUNTRY

RULE-47

Brittain, Jean H.

Pauly, John M.

Palo Alto Redwood City CA CA US US

US-CL-CURRENT: 324/309; 324/307, 324/318

Full Title Citation Front Review Classification Date Reference Sequences Attachments

Draw Desc Image

KWIC

2. Document ID: US 20020145042 A1

L22: Entry 2 of 14

File: PGPB

Oct 10, 2002

PGPUB-DOCUMENT-NUMBER: 20020145042

PGPUB-FILING-TYPE: new

DOCUMENT-IDENTIFIER: US 20020145042 A1

TITLE: Internet-based remote monitoring, configuration and service (RMCS) system capable of monitoring, configuring and servicing a planar laser illumination and imaging (PLIIM) based network

PUBLICATION-DATE: October 10, 2002

INVENTOR-INFORMATION:

NAME	CITY	STOT	COUNTRY	RULE-47
Knowles, C. Harry	Moorestown	NJ	US	
Schmidt, Mark C.	Williamstown	NJ	US	
Zhu, Xiaoxun	Marlton	NJ	US	
Defoney, Shawn	Runnemede	NJ	US	
Skypala, Edward	Blackwood	NJ	US	
Tsikos, Constantine J.	Voorhees	NJ	US	
Au, Ka Man	Philadelphia	PA	US	
Schwartz, Barry E.	Haddonfield	NJ	US	
Wirth, Allan	Bedford	MA	US	
Jankevics, Andrew	Westford	MA	US	
Good, Timothy A.	Clementon	NJ	US	
Ghosh, Sankar	Glenolden	PA	US	
Schnee, Michael D.	Aston	PA	US	
Kolis, George	Pennsauken	NJ	US	
Amundsen, Thomas	Turnersville	NJ	US	
Naylor, Charles A.	Sewell	NJ	US	
Blake, Robert	Woodbury Heights	NJ	US	
Dobbs, Russell Joseph	Cherry Hill	NJ	US	
Yorsz, Jeffery	Winchester	MA	US	
Giordano, Patrick A.	Blackwood	NJ	US	
Colavito, Stephen J.	Brookhaven	PA	US	
Wilz, David W. SR.	Sewell	NJ	US	
Svedas, William	Deptford	NJ	US	
Kim, Steven Y.	Cambridge	MA	US	
Fischer, Dale M.	Voorhees	NJ	US	
Tassell, Jon Van	Winchester	MA	US	

US-CL-CURRENT: 235/462.01

Full	Title	Citation	Front	Review	Classification	Date	Reference	Sequences	Attachments	KWIC
Draw	Desc	lmage								
y		***************************************							·····	***************************************
	3.	Documer	nt ID:	US 200	20140423	A 1				

File: PGPB

PGPUB-DOCUMENT-NUMBER: 20020140423

PGPUB-FILING-TYPE: new

L22: Entry 3 of 14

DOCUMENT-IDENTIFIER: US 20020140423 A1

TITLE: Moving table MRI with frequency-encoding in the z-direction

PUBLICATION-DATE: October 3, 2002

INVENTOR-INFORMATION:

NAME CITY STATE COUNTRY RULE-47

Brittain, Jean Helen Menlo Park CA US

US-CL-CURRENT: 324/301; 324/309

	FUH 1170	e Citation	riont F	teniem c	lassification	Date	Reference	sequences	Attacriments	KWUC
	Drawi Desc	Image								
		ia- i								
Y	***************************************	***************************************	***************************************	***************************************	***************************************	***************************************	***************************************		***************************************	***************************************

Oct 3, 2002

L22: Entry 4 of 14

File: PGPB Aug 22, 2002

PGPUB-DOCUMENT-NUMBER: 20020115929

PGPUB-FILING-TYPE: new

DOCUMENT-IDENTIFIER: US 20020115929 A1

TITLE: Magnetic resonance imaging for a plurality of selective regions set to object

continuously moved

PUBLICATION-DATE: August 22, 2002

INVENTOR-INFORMATION:

NAME

CITY

STATE

COUNTRY

RULE-47

Machida, Yoshio

Nasu-Gun

JΡ

US-CL-CURRENT: 600/410

Full Title Citation Front Review Classification Date Reference Sequences Attachments Oraw. Desc Image

KWIC

5. Document ID: US 6490476 B1

L22: Entry 5 of 14

File: USPT

Dec 3, 2002

US-PAT-NO: 6490476

DOCUMENT-IDENTIFIER: US 6490476 B1

TITLE: Combined PET and X-ray CT tomograph and method for using same

DATE-ISSUED: December 3, 2002

INVENTOR-INFORMATION:

NAME

CITY

STATE

ZIP CODE

COUNTRY

Townsend; David W.

Pittsburg

PA

Nutt; Ronald

Knoxville

TN

US-CL-CURRENT: 600/427; 250/363.03, 250/363.04, 378/4, 600/431, 600/436

Full Title Citation Front Review Classification Date Reference Sequences Attachments Draw, Desc Image

KWC

6. Document ID: US 6485413 B1

L22: Entry 6 of 14

File: USPT

Nov 26, 2002

US-PAT-NO: 6485413

DOCUMENT-IDENTIFIER: US 6485413 B1

TITLE: Methods and apparatus for forward-directed optical scanning instruments

DATE-ISSUED: November 26, 2002

INVENTOR - INFORMATION:

NAME CITY STATE CODE COUNTRY

Boppart; Stephen A. Boston MA Tearney; Gary J. Cambridge MA Bouma; Brett E. Boston MA Brezinski; Mark E. Malden MA Fujimoto; James G. Cambridge MA Swanson; Eric A. Acton MA

US-CL-CURRENT: 600/160; 600/129, 600/477, 600/478

Full Title Citation Front Review Classification Date Reference Sequences Attachments KMC

7. Document ID: US 6301497 B1

L22: Entry 7 of 14

File: USPT

Oct 9, 2001

US-PAT-NO: 6301497

DOCUMENT-IDENTIFIER: US 6301497 B1

TITLE: Method and apparatus for magnetic resonance imaging intersecting slices

DATE-ISSUED: October 9, 2001

INVENTOR-INFORMATION:

NAME CITY STATE ZIP CODE COUNTRY

Neustadter; David Maier D.N. Sharon Tichon IL

US-CL-CURRENT: 600/410; 128/920, 324/309

Full Title Citation Front Review Classification Date Reference Sequences Attachments KMC |
Draw, Description Image

8. Document ID: US 6275721 B1

L22: Entry 8 of 14 File: USPT Aug 14, 2001

US-PAT-NO: 6275721

DOCUMENT-IDENTIFIER: US 6275721 B1

TITLE: Interactive MRI scan control using an in-bore scan control device

DATE-ISSUED: August 14, 2001

INVENTOR-INFORMATION:

NAME CITY STATE ZIP CODE COUNTRY

Darrow; Robert David Scotia NY

Dumoulin; Charles Lucian London GB

Hardy; Christopher Judson Schenectady NY

US-CL-CURRENT: 600/410; 324/318, 600/411

Full Title Citation Front Review Classification Date Reference Sequences Attachments KMC

Drawi Desc Image

9. Document US 6161031 A

L22: Entry 9 of 14 File: USPT Dec 12, 2000

US-PAT-NO: 6161031

DOCUMENT-IDENTIFIER: US 6161031 A

TITLE: Optical imaging methods DATE-ISSUED: December 12, 2000

INVENTOR-INFORMATION:

NAME

CITY

STATE ZIP CODE COUNTRY

Hochman; Daryl

Edmonds

WA

Haglund; Michael M.

Seattle

WA

US-CL-CURRENT: 600/407; 128/922, 600/310, 600/475, 600/477

Title Citation Front Review Classification Date Reference Sequences Attachments KWIC Draw, Desc Image

10. Document ID: US 5845639 A

L22: Entry 10 of 14

File: USPT

Dec 8, 1998

US-PAT-NO: 5845639

DOCUMENT-IDENTIFIER: US 5845639 A

TITLE: Optical imaging methods

DATE-ISSUED: December 8, 1998

INVENTOR - INFORMATION:

NAME

CITY

STATE

ZIP CODE COUNTRY

Hochman; Daryl

Haglund; Michael M.

Edmonds Seattle WA WA

US-CL-CURRENT: 600/407; 356/39, 600/473, 600/476

Full Title Citation Front Review Classification Date Reference Sequences Attachments Drawi Desc Image

KWIC

11. Document ID: US 5761331 A

L22: Entry 11 of 14

File: USPT

Jun 2, 1998

US-PAT-NO: 5761331

DOCUMENT-IDENTIFIER: US 5761331 A

TITLE: Method and apparatus for tomographic imaging and image reconstruction using recombinant transverse phase differentials

DATE-ISSUED: June 2, 1998

INVENTOR-INFORMATION:

NAME

CITY

STATE ZIP CODE COUNTRY

Clark, III; William T.

Folsom

US-CL-CURRENT: 382/131; 378/4, 382/132, 382/254

KWIC

12. Document ID: US 5465718 A

L22: Entry 12 of 14

File: USPT

Nov 14, 1995

US-PAT-NO: 5465718

DOCUMENT-IDENTIFIER: US 5465718 A

TITLE: Solid tumor, cortical function, and nerve tissue imaging methods and device

DATE-ISSUED: November 14, 1995

INVENTOR-INFORMATION:

Haglund; Michael M.

NAME

CITY

STATE

ZIP CODE

COUNTRY

Hochman; Daryl

Edmonds Seattle

WA WA 98020

98133

US-CL-CURRENT: 600/420; 348/164, 348/68, 348/77, 600/431, 600/473, 600/476, 600/554

Full Title Citation Front Review Classification Date Reference Sequences Attachments

Draw, Desc Image

13. Document ID: US 5261404 A

L22: Entry 13 of 14

File: USPT

Nov 16, 1993

KWAC

US-PAT-NO: 5261404

DOCUMENT-IDENTIFIER: US 5261404 A

TITLE: Three-dimensional mammal anatomy imaging system and method

DATE-ISSUED: November 16, 1993

INVENTOR-INFORMATION:

NAME

CITY

STATE

ZIP CODE

COUNTRY

Mick; Peter R.

Kinnelon

NJ

07405

Savet; Mark

New York

NY

10022

US-CL-CURRENT: 600/425; 128/916, 600/160

Full Title Citation Front Review Classification Date Reference Sequences Attachments

Draw Desc Image

KWIC

14. Document ID: US 4995394 A

L22: Entry 14 of 14

File: USPT

Feb 26, 1991

US-PAT-NO: 4995394

DOCUMENT-IDENTIFIER: US 4995394 A

TITLE: Fast NMR cardiac profile imaging

DATE-ISSUED: February 26, 1991

INVENTOR-INFORMATION:

NAME

CITY

STATE ZIP COD

COUNTRY

Cline; Harvey E.

Schenectady,

NY

NY

Hardy; Christopher J.

Schenectady,

NY

US-CL-CURRENT: 600/410; 324/309

Full Tit	e Citation	Front	Review	Classification	Date	Reference	Sequences	Attachments
Draw, Desc	tmage							

KWIC

Generate Collection Print

Term	Documents
"WITHOUT STOPPING".DWPI,TDBD,EPAB,JPAB,USPT,PGPB.	0
MOVE.DWPI,TDBD,EPAB,JPAB,USPT,PGPB.	1417859
MOVES.DWPI,TDBD,EPAB,JPAB,USPT,PGPB.	898278
MOVING.DWPI,TDBD,EPAB,JPAB,USPT,PGPB.	1433698
MOVINGS.DWPI,TDBD,EPAB,JPAB,USPT,PGPB.	67
MOVED.DWPI,TDBD,EPAB,JPAB,USPT,PGPB.	1346067
MOVEDS.DWPI,TDBD,EPAB,JPAB,USPT,PGPB.	6
MOTION.DWPI,TDBD,EPAB,JPAB,USPT,PGPB.	692086
MOTIONS.DWPI,TDBD,EPAB,JPAB,USPT,PGPB.	61617
MOVEMENT.DWPI,TDBD,EPAB,JPAB,USPT,PGPB.	1715665
MOVEMENTS.DWPI,TDBD,EPAB,JPAB,USPT,PGPB.	213354
(L21 AND ((CONTINUOUS\$3 OR CONSTANT\$4 OR "WITHOUT STOPPING" OR CONVEY\$5) WITH (MOVE OR MOVING OR MOVED OR MOTION OR MOVEMENT))). USPT,PGPB,JPAB,EPAB,DWPI,TDBD.	14

There are more results than shown above. Click here to view the entire set.

Display Format: -

-

Change Format

Previous Page

Next Page

WEST

Generate Collection Print

L22: Entry 5 of 14

File: USPT

Dec 3, 2002

DOCUMENT-IDENTIFIER: US 6490476 B1

TITLE: Combined PET and X-ray CT tomograph and method for using same

Abstract Text (1):

A combined PET and X-Ray CT tomograph for acquiring CT and PET images sequentially in a single device, overcoming alignment problems due to internal organ movement, variations in scanner bed profile, and positioning of the patient for the scan. In order to achieve good signal-to-noise (SNR) for imaging any region of the body, an improvement to both the CT-based attenuation correction procedure and the uniformity of the noise structure in the PET emission scan is provided. The PET/CT scanner includes an X-ray CT and two arrays of PET detectors mounted on a single support within the same gantry, and rotate the support to acquire a full projection data set for both imaging modalities. The tomograph acquires functional and anatomical images which are accurately co-registered, without the use of external markers or internal landmarks.

Brief Summary Text (5):

This invention relates to a tomograph which has the capability of operating in either X-Ray computerized tomography (CT) or positron emission tomography (PET) mode. More specifically, it relates to a combined PET and CT scanner which allows co-registered CT and PET images to be acquired sequentially in a single device, overcoming alignment problems due to internal organ movement, variations in scanner bed profile, and positioning of the patient for the scan.

Brief Summary Text (7):

The role of PET imaging in oncology research and patient care is growing. The ability of PET to add unique functional information to that obtained by conventional anatomical-based modalities, such as CT and magnetic resonance (MR), is generating considerable interest. For space-occupying lesions in the head, chest, abdomen and pelvis, one of the best documented applications of PET is in the discrimination of benign from malignant causes. Thus far, .sup.18 F-fluorodeoxyglucose (FDG) has been used to image the distribution of glucose uptake in all of these applications. The increased glucose metabolism of the neoplasm has been used for several purposes. Specific applications include, among other things, determining the presence of recurrent glioma versus radiation necrosis, determining the presence of recurrent colon carcinoma versus surgical scar and radiation changes, determining the presence of pancreatic cancer versus pancreatitis, determining the presence of malignant solitary pulmonary nodules versus benign nodules, and determining the presence of metastatic lung carcinoma versus reactive lymph node.

Brief Summary Text (10):

Finally, the PET imaging of tumor masses, and particularly complex tumor masses with areas of cystic changes, necrosis, or surrounding edema, could potentially be used to guide diagnostic biopsies. In the head, this has been demonstrated to be fairly successful, but extracranial applications have not yet been studied systematically. While accuracy and reliability of CT-guided biopsies is high overall, typically greater than ninety percent (90%), it is known that this accuracy and reliability falls considerably to approximately eighty percent (80%) in the setting of complex lesions in presacral or retroperitoneal locations. Thus, functional knowledge of tumor metabolism would be helpful in better selecting an exact biopsy site in these conditions if correctly registered to CT data.

Brief Summary Text (11):

In recent years, there has been considerable progress in the development of techniques to co-register and align functional and anatomical images. This has been driven primarily by the demand for accurate localization of cerebral function visualized in PET studies where the low resolution morphology is, in most cases, insufficient to identify the related cerebral structures. Techniques to overcome this problem have been developed based, for example, on the identification of

certain geometrical features common to both imaging modelities. For example, A. C. Evans et al, J Cereb is od Flow Metab 11(2), A69-A78 (151) teach the use of landmark matching while D. G. Thomas et al, "Use of relocatable stereotactic frame to integrate positron emission tomography and computed tomography images: application to human malignant brain tumors, " Stereotactic and Functional Neurosurgery 54-55, 388-392 (1990) teach the use of externally-placed reference or fiducial markers. Identification of the skull and brain contour from either the PET transmission or emission scan and the MR or CT scan has also been employed as an alignment technique by C. A. Pelizzari et al, "Accurate three-dimensional registration of CT, PET and MR images of the brain, " J Comp Assist Tomogr 13, 2026 (1989). Following the identification of common structures in the two modalities, a rigid-body transformation is used to rotate and translate the MR or CT scan into the reference frame of the PET image, accounting for differences in pixel size between the two imaging modalities. A technique which uses a least squares approach to minimize the distribution of pixel-to-pixel ratios between the two images requiring alignment has proved successful both for PET to PET by R. P. Woods et al, "Rapid automated algorithm for aligning and reslicing PET images," J Comp Assist Tomogr 16, 620-633 (1992); and PET to MR by R. P. Woods et al, "MRI-PET registration with an automated algorithm," J Comp Assist Tomogr 17, 536-546 (1993). An interactive method has also been published U. Pietrzyk et al, "Three-dimensional alignment of functional and morphological tomograms," J Comp Assist Tomogr 14(1), 51-59 (1990), wherein a human observer makes alignment decisions based on visual inspection of images of brain sections displayed on a computer screen.

Brief Summary Text (13):

Essentially all the registration techniques mentioned above have been developed for use in cerebral studies, and in particular brain activation. This is to some extent because PET images of cerebral flow and metabolism already contain a limited amount of low-resolution anatomical information which can be effectively exploited by the alignment procedures. However, the problems of alignment and coregistration in other regions of the human body are more difficult to solve owing to the absence of even low-resolution morphology in the functional image. This is particularly acute in the abdomen, where the PET emission scan shows little or no anatomical detail. Furthermore, the advantage of co-registering organs other than the brain has been recognized only recently, with, as described above, a rapid growth in the use of FDG in oncology.

Brief Summary Text (14):

It is evident, therefore, that in regions such as the thorax and abdomen, the demonstration of increased FDG uptake is limited in value without an unambiguous localization of tracer uptake to a specific structure (e.g. a tumor) seen on the corresponding CT image. It is desirable, therefore, to accomplish accurate registration of anatomical data, such as is obtained with CT, to improve the use of PET imaging in all of the above applications in oncology. In the discrimination of a benign versus a malignant mass, a CT scan typically defines the borders of the mass and co-registration with PET allows a more accurate quantitative evaluation. In certain organs, where nearby structures have a high concentration of excreted tracers, such as FDG in the renal pelvis, exact registration of PET and CT allows a finer discrimination of the etiology of a "hot spot", thus reducing the likelihood of falsely identifying the mass as a tumor, or misjudging a focal accumulation of tracer as probable urine activity. For future tracers which may have labeled metabolites excreted via the hepatobiliary system and bowel this may be even more crucial.

Brief Summary Text (15):
In "`Anatometabolic` tumor imaging: fusion of FDG PET with CT or MRI to localize foci of increased activity, "J. Nucl. Med. 34, 1190-1197 (1993), R. L. Wahl et al. disclose the alignment of CT scans with PET FDG functional images and have thus demonstrated the importance of combining anatomy and function in organs other than the brain. Wahl et al. concentrated on tumors in the thoracic and abdominal regions using both external markers and, in the thorax, internal anatomical landmarks such as the carina. Functional and anatomical images were aligned to within an error of magnitude of 5-6 mm, allowing more precise information to be obtained on the extent of the tumoral involvement of surrounding soft tissues than would have been possible from the PET scan alone. This work has also highlighted the difficulties of aligning organs which are not rigidly attached within the body. While the brain remains fixed in the skull, the position of organs such as the liver may depend upon the precise way in which the patient lies on the bed. Thus, PET-CT post-hoc alignment may be affected by different internal relationships and deformations within the body, limiting the accuracy of such an approach.

Brief Summary Text (16):

As is well-known, compared to anatomical imaging modalities, SPECT images are

2 of 16 01/29/2003 9:41 AN photon-limited and generally lack anatomical landmarks, was making image alignment, and the definition of lions-of-interest, even more of problem than it is for PET. In addition, non-uniform photon attenuation introduces distortions and artifacts into the reconstructed images. A prototype hybrid CT/SPECT scanner has been developed to address these issues. As discussed by T. F. Lang et al., "A prototype emission-transmission imaging system," IEEE Nucl. Sci. Symposium Conf. Record 3, 1902-1906 (1991); and T. F. Lang et al., "Description of a prototype emission-transmission computed tomography imaging system, "J. Nucl. Med. 33, 1881-1887 (1992), this device employs the same one-dimensional array of highpurity germanium detectors for both CT and single photon imaging. A goal of the CT/SPECT project is also to use the X-ray CT image to provide the attenuation factors to correct the SPECT data, as suggested by J. S. Fleming, "A technique for using CT images in attenuation correction and quantification in SPECT, " Nucl. Med. Commun 10, 83-97 (1989). The use of CT images for attenuation correction had been originally proposed by S. C. Moore, "Attenuation compensation" in Ell, P. J. et al., Computed Emission Tomography, London, Oxford University Press, 339-360 (1982). The 100 kVp X-ray source is capable of producing a dual-energy X-ray beam, such that an energy-corrected attenuation map can be obtained for use with the radionuclide data, as disclosed by B. H. Hasegawa et al, "Object specific attenuation correction of SPECT with correlated dual-energy X-ray CT, " IEEE Trans. Nucl. Sci. NS-40 (4), 1242-1252 (1993). Operating the device with two energy windows also allows simultaneous emission-transmission acquisitions to be performed, although the authors report a certain level of contamination of the emission scan by the transmission X-ray beam. This disclosure demonstrates the potential of a device capable of performing both anatomical and functional measurements. It has also given rise to a detailed simulation study to investigate the different techniques for scaling the attenuation coefficients from CT energies (50-80 keV) to SPECT (140 keV). See K. J. LaCroix et al, "Investigation of the use of X-ray CT images for attenuation compensation in SPECT, " IEEE 1993 Medical Imaging Conference Record (1994).

Brief Summary Text (17):

While the attenuation correction for PET is of a greater magnitude than for SPECT, it is theoretically-more straightforward. However, since it is generally based on patient measurements (a transmission scan), it introduces additional noise into the reconstructed emission scan. In practice, in order to limit the duration of the PET scan procedure, abdominal transmission scans of 10-15 minutes are typical, during which 100 million counts are acquired (.about.3 million per slice, or 100 counts per coincidence line of response, i.e. a 10% statistical accuracy), which introduces significant noise into the corrected emission scan. In practice, only lines-of-response (LOR's) through the patient contain useful transmission information, and since some of the coincidence events will lie in LOR's which do not pass through the patient, the total useful counts in a transmission scan is often less than 100 million. In addition, patient movement between the transmission and emission scan (which may be acquired 40 minutes or so later) can introduce serious artifacts and distortions into the reconstructed image, as disclosed by S. C. Huang et al, "Quantitation in positron emission tomography: 2. Effects of inaccurate attenuation correction, " J Comput Assist Tomogr 3, 804-814 (1979).

Brief Summary Text (18):

FIGS. 1A and 1B illustrate a PET transmission image and a CT image, respectively, for the same transaxial section through a patient. As illustrated in these figures, the statistical noise in a CT image is considerably less than that in an image formed from a PET transmission scan, due to the much higher photon flux available in CT scans. A CT image is formed from a photon flux equivalent to 10.sup.10 -10.sup.11 photons, compared with the .about.10.sup.6 photons/slice in a PET transmission scan.

Brief Summary Text (19):

In a typical PET transmission scanning procedure, the PET transmission scan is performed pre-injection, while the emission scan is performed 45 minutes post-injection, which is potentially a significant source of error if there is any patient motion during this period.

Brief Summary Text (24):

The second and more technically-challenging approach, is to acquire the CT image at two different photon energies--for example, 40 keV and 80 keV--and use these data to extract the individual photoelectric and Compton contributions to .mu..sub.E (x). See R. E. Alvarez et al, "Energy-selective reconstructions in X-ray computerized tomography," Phys Med Biol 21(5), 733-744 (1976); and D. E. Avrin et al, "Clinical applications of Compton and photo-electric reconstruction in computed tomography: preliminary results," Invest Radiol 13, 217-222 (1978). The different contributions are then scaled in energy separately. The Compton contribution decreases linearly

while the photoelectric contribution decreases rapidly 1/E.sup.3. The two separate contributions in be scaled independently and bined to form a monoenergetic attenuation map at 140 keV as shown by Hasegawa et al. for a prototype SPECT/CT detector block. Dual-energy CT is an accurate technique for determining the Compton and photoelectric contributions in these energy ranges, but the extrapolation of the monoenergetic attenuation map to 511 keV is not readily apparent. Additionally, the formation and detection of two CT spectra is technically challenging, requiring either the mechanical switching of foil filters, or the switching of the X-ray tube accelerating voltage, which is limited by the possibility of overheating. It also generally requires a complex calibration procedure.

Brief Summary Text (25):

The development of 3D PET has resulted in the acquisition of PET data with a significant fraction of scattered events. This is because the role of the septa, which are retracted during a 3D acquisition, is primarily to shield the detectors from out-of-plane scatter. The absence of shielding is reflected in a factor of three increase in scatter, from 10%-15% of the total events collected in 2D with septa extended, to 40%-45% in 3D with the septa retracted. This increase has served to focus attention on the problem of scatter correction in PET. However, even in 2D, for accurate quantitation, the scatter background of 10%-15% must be subtracted. The non-negligible scatter contribution in 2D PET comes mainly from in-plane scatter, and is a consequence of the poor energy resolution of the BGO block design. Loss of light in the block results in a decrease in energy resolution from an intrinsic 11% to as much as 23% in a block design. PET scanners are therefore operated with a lower energy threshold set typically between 250 keV and 350 keV to minimize the rejection of unscattered photons. At such a threshold, photons which lose only a small amount of energy by scattering, and are hence deviated through a small angle, are accepted as true, photopeak events. Application of an energy threshold therefore results in the preferential selection of the more forward-peaked component of the energy spectrum.

Brief Summary Text (28):

In 3D, the increased amounts of scatter demand an accurate correction procedure to improve contrast, without losing the quantitation which is a unique feature of PET. S. R. Cherry et al., "Correction and characterization of scattered events in three dimensional PET using scanner with retractable septa, " J Nucl Med 34, 671-678 (1993), have proposed the use of an auxiliary 2D scan from which the scatter distribution in 3D can be estimated. Following the Bergstrom-type approach, D. L. Bailey et al., "A convolution-subtraction scatter correction method for 3D PET," Phys Med Biol 39, 412-424 (1994), investigated a convolution-subtraction method to correct for scatter. The scatter kernel is modeled as a monoexponential function of the form k.sup.(-b.vertline.x.vertline.), where k is the scatter ratio (scatter/trues) and b is the slope of the tails of the scatter distribution. The parameters k and b are obtained from line source measurements in an appropriate phantom (e.g. a 20 cm diameter uniform cylinder), and x is then the distance from the line source. The procedure is iterative, such that in the first step the scatter is obtained from the convolution of the measured projection data with the scatter kernel. This scatter estimate is then subtracted from the measured projections. However, this first step will tend to overcorrect because the measured projection data used in the convolution includes scatter. In subsequent iterations, the kernel is convolved with the measured projection data after subtraction of scatter estimated from the previous step. Usually, 3-4 iterations are sufficient. A recent improvement to this method (Bailey et al.) has been the introduction of a spatially-variant scatter ratio (k(x)), based on geometrical information obtained from the PET transmission scan. This approach may therefore be improved by use of the CT scan rather than the PET transmission scan. A second approach taken by D. Gagnon et al., "Introduction to holospectral imaging in nuclear medicine for scatter subtraction," IEEE Trans Med Imaging 8(3), 245-250 (1989), which has been evaluated for scatter correction in 3D PET, is based on the use of multiple energy windows, a procedure that has its origins in single photon tomography. In this approach, data is simultaneously collected in more than one energy window, and the information from other windows is used to estimate the scatter within the photopeak window. State-of-the art PET scanners have the capability to acquire data in two energy windows, and two different implementations of a dual energy window scatter correction have been proposed. The first, studied by S. Grootoonk et al., "Correction for scatter using a dual energy window technique with a tomograph operating without septa." IEEE 1991 Medical Imaging Conference Record, 1569-1573(1992), sets a lower energy window which is assumed to contain predominantly scatter. Data collected in this lower window are then scaled to provide an estimate of the scatter contribution in the photopeak window, where the scaling factors are obtained from line source measurements in air and phantoms. A second dual-energy window approach, the Estimation of Trues Method due to B.

Bendriem et al., "A Proscatter correction using simultations with low and high lower energy resholds," IEEE 1993 Medical Intended in Conference Record 3, 1779-1783 (1994), sets an upper window with a very high (650 keV) lower threshold such that it contains only true coincidences. Again, the information in this window is used to estimate the contribution of true coincidences in the photopeak window. This approach has the advantage that the estimate in the upper window does not depend upon the scattering medium since it contains only true coincidences. Statistical noise may be a problem, however, due to the small number of counts collected in this upper window. In contrast to the convolution-subtraction method, the dual-energy window approach can in principle take into account scatter from activity outside the field-of-view, at least to the extent to which this information is contained in the lower energy window. For the method of Grootoonk et al., efforts are also being made to incorporate spatial information based on the PET transmission scan.

Brief Summary Text (29):

A third method investigated by J. M. Ollinger is to directly model the scatter using the Klein-Nishina equation describing Compton scattering. This method is disclosed in Ollinger, J. M., "Model-based scatter correction for fully 3D PET," Phys Med Biol. 41(1), 153-176, (1996), In this approach, the tracer distribution is obtained from a reconstruction uncorrected for scatter, and the geometry of the scattering medium is obtained from the PET transmission image. The expected distribution of scatter in the projections is then calculated using the Klein-Nishina equation which gives the probability of a photon scattering through a particular angle. Such an approach obviously involves considerable computational effort, and an efficient implementation has been developed by Ollinger which is capable of estimating the distribution of scatter in the projections within a few minutes on a fast processor. Detailed Monte Carlo simulations of scatter yield a generally low-frequency background with few features of the underlying tracer distribution or scattering medium. Therefore, it is sufficient to model such a slowly-varying distribution at a lower spatial resolution than the measured projection data, thereby considerably reducing computation time. Again, since this method has no information concerning activity outside the field-of-view, the calculated scatter distribution will not in general correct for such an eventuality. Watson et al. have independently developed a similar approach to Ollinger based on a single scatter model, as disclosed in Watson, C. C., D. Newport, and M. E. Casey, "A single scatter simulation technique for scatter correction in 3D PET" in: Grangeat P and J-L Amans, Three Dimensional Image Reconstruction in Radiology and Nuclear Medicine., Dordrecht. Kluwer Academic. 255-268 (1996).

Brief Summary Text (31):

One possibility that arises when anatomical CT data is accurately co-registered with functional PET data is to use the CT image to constrain the PET image reconstruction. A maximum .alpha. posteriori (MAP) method has been explored with co-registered PET and MR images by R. Leahy et al., Incorporation of anatomical MR data for improved functional imaging with PET," Information Processing in Medical Imaging, XIIth IPMI International Conference, Wye, UK, 105-120. (1991); X. Yan et al., "MAP estimation of PET images using prior anatomical information from MR scans," IEEE 1992 Medical Imaging Conference Record 2, 1201-1203 (1993); and others. Promising results from simulation studies by Z. Zhou, et al., "A comparative study of the effects of using anatomical priors in PET reconstruction," IEEE 1993 Medical Imaging Conference Record 3, 1749-1753 (1994), show that incorporation of prior anatomical boundary information into the MAP reconstruction process can significantly reduce bias and noise in images. This was based on comparisons of the MAP-based reconstructions to those produced by other reconstruction methods, including filtered-back-projection and standard expectation-maximization (EM).

Brief Summary Text (33):

Therefore, it is an <u>object</u> of the present invention to provide a means for using CT <u>images</u> as a basis for the attenuation correction of PET data in order to reduce the increased statistical noise in the PET <u>image</u> due to the PET transmission scan.

Brief Summary Text (34):

It is a further <u>object</u> of the present invention to provide such a means whereby a rapid, post-injection, transmission scan is performed immediately before and/or during the PET emission scan so as to minimize the effects of <u>patient movement</u>.

Brief Summary Text (35):

Another <u>object</u> of the present invention is to provide a combined PET and X-Ray CT tomograph capable of combined functional and anatomical <u>imaging</u>.

Brief Summary Text (36):

A further object of the present invention is to provide such a device which is

capable of co-registra on of images for any organ in a part of the body.

Brief Summary Text (39):

In accordance with the teachings of the present invention, an X-ray CT and PET tomograph having a physically known relationship one with the other. Each of the X-ray CT and PET tomograph are configured for use with a single patient bed such that a patient may be placed on the bed and moved into position for either or both of an X-ray CT scan and a PET scan. This may be accomplished in a first instance wherein X-ray CT detectors and PET tomograph detectors being disposed within a single gantry, and wherein a patient bed is movable therein to expose a selected region of the patent to either or both scans. In a second instance, the X-ray CT and PET tomograph detectors are disposed in separate gantries which are fixed relative to each other, and wherein the patient bed is movable between the gantries. In a third instance, the X-ray and PET tomograph detectors are disposed in separate gantries, either of which is movable with respect to the other, wherein the patient bed is movable with respect to each gantry

Brief Summary Text (40):

The tomograph acquires functional and anatomical images which are accurately co-registered, without the use of external markers or internal landmarks. A secondary objective is to use the CT data to improve the correction of the PET data for attenuation and for contamination from scattered photons. By using the CT image in this manner, low-noise attenuation correction factors for PET are generated, and by integrating the anatomical information from the CT into scatter correction methods, an accurate scatter correction is obtained.

Drawing Description Text (2):

The above-mentioned features of the invention will become more clearly understood from the following detailed description of the invention read together with the drawings in which:

Drawing Description Text (3):

FIG. 1A illustrates a PET transmission image for a transaxial section through a patient;

Drawing Description Text (4):

FIG. 1B illustrates a CT image of the same transaxial section of FIG. 1A, showing reduced noise and increased contrast compared with the corresponding PET transmission image of FIG. 1A;

Drawing Description Text (5):

FIG. 2A is a schematic diagram of the side view of the PET/CT scanner of the present invention showing the CT scanner and PET scanner disposed within a single gantry;

Drawing Description Text (6):

FIG. 2B illustrates an alternate embodiment wherein the X-ray CT and PET tomograph detectors are disposed in separate gantries which are fixed relative to each other and the patient bed is movable between the gantries;

Drawing Description Text (7):

FIG. 2C illustrates a further alternate embodiment wherein the X-ray and PET tomograph detectors are disposed in separate gantries, either of which is movable with respect to the other, and wherein the patient bed is movable with respect to each gantry;

Drawing Description Text (9):

FIG. 4A illustrates a central transaxial section of a transmission image of the thorax of a normal volunteer acquired for 3 min per bed position using dual 30 MBq germanium rod sources;

Drawing Description Text (10):

FIG. 4B illustrates the central transaxial section of a transmission image of the thorax of FIG. 4A of a normal volunteer <u>acquired</u> for 3 min per <u>bed</u> position using dual 550 MBq cesium point sources;

Drawing Description Text (12):

FIG. 5B illustrates the scaled attenuation map of the CT image of FIG. 5A calculated using the hybrid segmentation and scaling method and smoothed to match the resolution of the PET data;

Drawing Description Text (14):

FIG. 6A illustrates the transmission images of a transverse section through a whole-body phantom acquired using the CT scanner;

Drawing Description Te (15):

FIG. 6B illustrates the transmission images of the same transverse section of FIG. 6A through a whole-body phantom acquired using the cesium sources in singles mode;

Detailed Description Text (2):

A combined PET and X-Ray CT tomograph, constructed in accordance with the present invention, is illustrated generally as 10 in the figures. The combined PET and X-Ray CT tomograph, or PET/CT scanner 10 allows registered CT and PET images to be acquired sequentially in a single device, overcoming alignment problems due to internal organ movement, variations in scanner bed profile, and positioning of the patient for the scan. In order to achieve good signal-to-noise (SNR) for imaging any region of the body, an improvement to both the CT-based attenuation correction procedure and the uniformity of the noise structure in the PET emission scan is provided.

<u>Detailed Description Text</u> (3):

In the described embodiment, the PET/CT scanner 10 combines a Siemens Somatom AR.SP spiral CT scanner 12 with a rotating ECAT ART PET scanner 14. The PET/CT scanner 10 includes a PET scanner 14 and a CT scanner 12, both commercially-available, in a physically known relationship one with the other. Each of the X-ray CT scanner 12 and the PET scanner 14 are configured for use with a single patient bed 18 such that a patient may be placed on the bed 18 and moved into position for either or both of an X-ray CT scan and a PET scan.

Detailed Description Text (4):

In the illustrated embodiment of FIG. 2A, the completed PET/CT scanner is shown having X-ray CT detectors 12 and PET tomograph detectors 14 being disposed within a single gantry 16, and wherein a patient bed 18 is movable therein to expose a selected region of the patent to either or both scans. For testing, a Somatom AR.SP (spiral) CT scanner, manufactured by Siemens in Erlangen, Germany, and an ECAT ART PET tomograph, manufactured by CTI PET Systems (Knoxville, Tenn., USA) and distributed through Siemens, were used. The two systems are combined by mounting the ECAT ART components onto the rear of the AR.SP on a common rotating support.

Detailed Description Text (5):

In a second instance, illustrated in FIG. 2B, the X-ray CT and PET tomograph detectors 12,14 are disposed in separate gantries 16A,B which are fixed relative to each other, and wherein the patient bed 18 is movable between the gantries 16A,B. In a third instance, illustrated in FIG. 2C, the X-ray and PET tomograph detectors 12,14 are disposed in separate gantries 16A',B', either of which is movable with respect to the other, wherein the patient bed 18' is movable with respect to each gantry 16A',B', as indicated by the arrows 20. Alternatively, one or both gantries 16A',B' may be moved relative to the patient bed 18' and the other of the gantries 16A',B' as indicated by the arrow 22. In each of these embodiments as illustrated in FIGS. 2A-2C, it is shown that the patient is placed on a single patient bed 18 for either or both scans, with either or all of the scanning devices and the patient bed is/are moved to accomplish the required scan(s).

Detailed Description Text (6):

The PET/CT scanner of the illustrated embodiment rotates at 30 rpm and is housed within a single gantry with dimensions of 168 cm high and 170 cm wide. The patient entry port defines a diameter of 60 cm and a tunnel length of 110 cm. The CT aperture is at the front of the scanner and the PET imaging volume is at the rear. The center of the PET volume is displaced 60 cm axially from the center of the CT slice. A set of contiguous spiral CT scans of a whole-body is acquired in two to three minutes as the patient bed moves continuously through the scanner. The PET scan is acquired in multi-bed mode with data acquisition lasting up to ten minutes at each bed position. Depending on the number of bed positions required to cover the region to be scanned, the complete PET scan may take forty to fifty (40-50) minutes, in addition to the forty-five to sixty (45-60) minute uptake period. The PET/CT scanner of this embodiment has the capability to scan a combined axial length of up to 100 cm by both modalities. While specific dimensions and lengths are described herein, it will be understood that these dimensions are for illustration purposes only and are not intended as limitations of the present invention.

Detailed Description Text (7):

The CT scan is acquired before the PET scan, following a sixty (60) minute uptake period after .sup.18 F-FDG activity has been injected into the patient. No degradation of the CT image is observed due to the activity in the patient. The CT images are reconstructed on the CT acquisition computer and then transferred to the PET console. The CT images are used to generate the attenuation correction factors. Specifically, the attenuation image at 511 keV is estimated by first using a

threshold to separate at the bone component of the CT age, and then using separate scaling facts for the bone and non-bone component. These factors are applied after scatter correction to the PET emission data to correct for attenuation, and the PET images are then reconstructed using a Fourier rebinning technique (FORE) and then independently by the ordered-subset EM (OSEM) iterative reconstruction algorithm (FORE+OSEM).

Detailed Description Text (10):

where the scanner has been calibrated to yield tissue concentration in the tumor ROI in absolute units of radioactive concentration (MBq/ml). The expression may be modified to use the lean body weight to account for the uptake of .sup.18 F-FDG primarily into muscle rather than fat. SUV has been used to distinguish significant uptake in malignant tissue from uptake in a normal or non-malignant process by adopting a threshold--an SUV greater than a particular value (e.g. 2.5) is suggestive of a malignant process. Glucose level, time after injection, ROI size and scanner resolution are fixed when performed on the PET/CT. Plasma glucose levels are checked by obtaining a 1 ml blood sample at the end of the patient scan.

Detailed Description Text (11):

The images are displayed with the PET adjacent to the corresponding CT sections, and also as fused PET and CT images. The display tool allows the physicians reading the images to scan through the volume, viewing either the fused images or the PET and CT images separately with a linked cursor. The PET images are scaled in SUV values.

<u>Detailed Description Text</u> (12):

The PET images are therefore fully quantitative and are interpolated and displayed with the same pixel size as the CT images. PET images are displayed either adjacent to, or superimposed on, CT images for simultaneous interpretation of functional and morphological information. In one embodiment, the PET and CT images are displayed side by side in a viewing tool with linked cross-hair cursors, so that positional correspondence between the two image sets is easily established. A second technique of image `fusion` is also employed, where the two different image sets are combined into a single image. See FIG. 3. For display of the fused PET and CT images, an alternating pixel method is extended to a 3D display format. Since the PET images have an isotropic resolution of approximately 10 mm for whole-body oncology imaging, the images are interpolated into the CT image space without loss of information in the PET image, thus preserving the resolution of the CT image. Because image fusion methods can obscure low-contrast objects, the CT display panel can be toggled between CT only and fused PET/CT mode. The viewing panels also have independent color scales and can be switched between transverse, sagittal, and coronal viewing modes.

Detailed Description Text (13):

The fused image display offers a two-dimensional, slice-byslice approach to the display of a three-dimensional volume data set. In order to offer a fully 3D approach to the data, and enhance the display capabilities of the PET/CT, a 3D display computer is added to the CT scanner. The 3D display computer offers interactive 3D shaded graphics of anatomical structures, displayed as shaded surfaces with or without transparency. The addition of functional structures, such as tumor masses, to the 3D anatomical framework has considerable diagnostic utility, with the 3D display computer providing the user with the ability to explore the functional anatomy of the human body fully in three dimensions.

<u>Detailed Description Text</u> (14):

The CT scanner used for testing in the combined PET/CT design is a third generation spiral, or helical, CT tomograph. A number of design parameters of the Somatom AR.SP are as follows:

<u>Detailed Description Text</u> (15):

The AR.SP used has a metal ring M-CT 141 tube that produces X-ray spectra of 110 kV.sub.P and 130 kV.sub.P with a 6.5 mm Al-equivalent filter. The tube is operated with a flying spot, which doubles the number of detector position readouts to 1024 from 512 xenon gas-filled Quantillarc detector chambers. The X-ray tube, detectors and most of the data processing system of the CT are mounted on the rotating support driven by a synchronous motor.

Detailed Description Text (16):

The standard ECAT ART (PET) scanner comprises dual arrays of BGO block detectors. Each array consists of 11 blocks disposed in a transaxial direction by 3 blocks disposed axially, covering an arc of approximately 83.degree. The detector arrays are not symmetrically opposed but are offset by approximately 15.degree. so as to increase the diameter of the transaxial FOV to 60 cm without requiring additional detector blocks. The ART has 46% of the detectors in the corresponding stationary,

full-ring scanner, the CAT EXACT. The detector blocks approximately 54 mm.times.54 mm.times.2 mm in size, cut into 8.times.8 stals each dimensioned to approximately 6.75 mm.times.6.75 mm.times.20 mm. The 8.times.8 crystal array is viewed by four photomultiplier tubes and Anger-type logic is used to localize the photon interactions within the block. The axial FOV is 16.2 cm, subdivided into 24 partial rings of detectors. Shielding from out-of-field activity is provided by arcs of lead, approximately 2.5 cm thick, mounted on both sides of the detector assembly and projecting approximately 8.5 cm into the FOV beyond the front face of the detectors.

Detailed Description Text (17):

The ECAT ART scanner has no septa and the detector arrays and shielding rotate continuously at 30 rpm to collect the full set of 3D projections required for image reconstruction. A complete 3D data set is acquired every two seconds. Continuous rotation eliminates the requirement for additional gantry cooling, and fans start automatically if, for any reason, gantry rotation is halted. An encoder monitors the position of the gantry during rotation, so that the acquired LOR's are assigned to the correct sinogram addresses. Power and serial communications to the rotating assembly are transmitted over mechanical slip rings, while high speed digital data transfer is by optical transmission.

Detailed Description Text (18):

In the standard ART scanner configuration, attenuation correction factors are obtained from a transmission scan performed with two rotating rod sources mounted at opposite ends of one detector array. In the PET/CT scanner of the present invention, dual 550 MBq .sup.137 CS collimated point sources are used to provide significantly improved transmission image quality with reduced scan duration. Using the cesium point sources, an additional approximately three (3) minutes per bed position is required for the transmission scan. The cesium singles sources provide an alternative to CT-based attenuation correction, and the combined PET/CT scanner has the capability of being operated in PET or CT mode independently, and can also acquire both types of transmission image allowing for a comparison to be made between the two approaches.

Detailed Description Text (20):

Standard performance measurements for CT scanners include the determination of attenuation values of air and water, in addition to image pixel noise and spatial resolution. Attenuation values for water were measured using the test protocol of the Somatom AR.SP. A 20 cm diameter water-filled cylinder was placed in the center of the transaxial FOV and tomograms were acquired at 110 kV.sub.P and 130 kV. Mean pixel value and standard deviation were calculated from a circular region-of-interest (ROI) covering 80% of the area of the water phantom. A similar measurement was performed with no object placed inside the FOY to determine the attenuation value of air. The values for air and water are defined to be -1000 HU and O HU, respectively, and should be independent of the X-ray tube voltage. Mean CT numbers were also determined from five circular ROI's, 4 cm in diameter, including a central ROI and four equally spaced peripheral ROI's. The absolute value of the difference between the average CT numbers of the central test ROI and the CT numbers of the four peripheral ROI's represents the homogeneity at 110 kV.sub.P and 130 kV.sub.P, respectively. The spatial resolution is determined by scanning an air-filled cylinder with a thin metal wire positioned parallel to the main scanner axis. The resolution is expressed in line pairs per cm. The results of these measurements for the CT components are summarized as follows: Transaxial spatial resolution [mm] 0.45 (at 1.9 s scan time)

Detailed Description Text (21):

No significant degradation of the performance of either the ECAT ART or the Somatom AR.SP was identified as a consequence of having the two devices mounted in the same gantry. Because the performance of BGO PET detectors is temperature-dependent, the PET/CT scanner was tested for potential temperature fluctuations inside the PET/CT gantry, and specifically for increases due to the operation of, and heat dissipated by, the X-ray tube. The temperature inside the gantry was measured during the CT operation and an increase of only 1.degree. C. was observed, too small to significantly affect the performance of the ART scanner. Results of the testing showed that the PET and CT components may be operated independently with identical performance to the standard Somatom and ECAT ART.

Detailed Description Text (23):

The PET/CT scanner is equipped with dual, collimated, cesium sources, each with an activity of 550 MBq. The point sources move in the axial direction to scan the full field-of-view. The collimators reduce the contribution from scattered photons. The high activity level of the cesium sources compared to the germanium rods results in a significant improvement in transmission image quality. This improvement is shown

in FIGS. 4A and 4B for transmission scan of the thorse of a normal volunteer. The scan duration of three 3) minutes was the same for both acquisitions. The superior image quality of the singles acquisition is evident from FIG. 4B, thus illustrating the comparison of an emission scan reconstructed with attenuation correction factors obtained from a point source transmission scan with the same emission scan reconstructed with CT-based attenuation correction factors, as will be described in further detail below.

Detailed Description Text (25):

The CT images are scaled from 70 keV to 511 keV in three steps (Kinahan et al., 1998). First, the CT image is divided into regions of pixels classified as either non-bone or bone by simple thresholding or more sophisticated segmentation methods. A threshold of 300 Hounsfield units (HU) gives acceptable results. Non-bone classified pixel values are then scaled with a single factor of 0.53, and bone classified pixel values are scaled with a lower scaling factor of 0.44. Finally, attenuation correction factors along oblique LOR's are obtained by forward projection through the segmented and scaled CT images. An illustrative example is shown in FIGS. 5A, 5B and 5C. The original CT image is shown in FIG. 5A, and the corresponding image after segmentation and scaling to 511 keV is shown in FIG. 5B. These figures illustrate the considerable detail that is preserved at the higher energy after scaling. Such detail is generally not visible on PET transmission images, illustrated in FIG. 5C, owing to the high level of statistical noise, even with cesium transmission sources.

Detailed Description Text (26):

The PET/CT scanner of the present invention, providing both a CT scan and a standard PET transmission scan with cesium sources, allows the two approaches to be compared, and the CT-based attenuation correction algorithm to be evaluated in patients. To illustrate such a comparison, FIG. 6A shows the CT image of a transverse section through a whole-body phantom with arms in the <u>field-of-view</u>, and FIG. 6B shows the corresponding transmission image of the same section obtained with the cesium sources.

Detailed Description Text (27):

As with patient studies, the arms are truncated on the CT scan owing to the smaller, 45 cm diameter, transaxial field-of-view of the scanner. For this simple phantom, the two images are comparable except for the truncation of the arms on the CT scan (FIG. 6A), and the increased statistical noise from the cesium transmission sources (FIG. 6B). The increase in noise is a result of the photon flux from the X-ray source, which is equivalent to an activity of 2.times.10.sup.8 MBq, compared to only 550 MBq in each of the cesium sources. The average .mu.-value for a region-of-interest 10 cm.times.2 cm in size in the "mediastinum" of the phantom is 0.097.+-.0.0003 cm.sup.-1 and 0.095.+-.0.007 cm.sup.-1 for the CT and the cesium source scan, respectively.

<u>Detailed Description Text</u> (28):

FIGS. 7A and 7B illustrate the corresponding emission scans reconstructed with CT-based attenuation correction, and the standard PET attenuation correction with the cesium sources, respectively. The two reconstructed emission images are similar, except for the presence of the arms in FIG. 7B. This is due to the larger transaxial field-of-view (FOV) of the cesium source transmission scan that matches the 60 cm diameter FOV of the PET emission scan. An ROI placed on the "mediastinum" of the reconstructed emission image has a mean value (in arbitrary units) of 8.9.+-.1.2 and 8.5.+-.1.4 for the CT-based (FIG. 6A) and cesium source-based (FIG. 6B) attenuation correction factors, respectively. The similarity of the variances on these means indicates that the dominant contribution to the noise in the study illustrated in FIGS. 7A and 7B originates from the photon statistics (noise) in the emission scan and not from the transmission scan.

Detailed Description Text (29):

Scatter correction for the PET emission scans is accomplished using a single scatter simulation algorithm which estimates the scatter contribution at any point in an emission projection view by integration of a scattering kernel over the volume of the scattering medium. The scattering medium is estimated from the PET transmission scan. This scatter correction model provides routine scatter correction of combined PET/CT studies by estimating the geometry and distribution of the scattering medium from the scaled CT image. FIGS. 8A and 8B illustrate the results of CT-based scatter correction for a thorax phantom study with hot and cold lesions simulated with spheres. CT-based attenuation correction was applied as described above. Compared to FIG. 8A, FIG. 8B shows that the CT-based scatter correction significantly reduces the scatter contribution in the cold lung region and improves the contrast in the cold spherical lesion positioned between the lungs, as illustrated by the arrow.

仁 (30): Detailed Description 7

Detailed Description 7 t (30):
In a further method for reconstructing PET images, Four rebinned PET data are reconstructed by minimizing a penalized weighted least-squares (PWLS) objective function, as disclosed by Fessler, J. A., "Penalized Weighted Least-Squares Image Reconstruction for Positron Emission Tomography," IEEE Trans Med Imaging, 13, 290-300 (1994). The penalty term of the objective function is a quadratic roughness penalty based on a 3D pixel neighborhood N, consisting of 26 adjacent neighbors. The penalty weights are derived from the anatomical (CT) data using voxel labels corresponding to the classification of the voxel. The weights are chosen to encourage smoothness inside, but not across, anatomical regions. For simplicity, the penalty weights are kept constant during reconstruction with FORE+PWLS, as shown by Comtat C., P. E. Kinahan, J. A. Fessler, T. Beyer, D. W. Townsend, M. Defrise, and C. Michel, "Reconstruction of 3D whole-body PET data using blurred anatomical labels," IEEE Medical Imaging Conference Record, CD-ROM (1999). Since in practice, mismatches between anatomical and functional data are unavoidable, the labels are "blurred" to reflect the uncertainty associated with the anatomical information. The images in FIGS. 9A, 9B and 9C illustrate the advantage of using CT-derived anatomical information in the PET image reconstruction. The contrast of the small lesion in the upper 'mediastinal' region (arrowed), in particular, is significantly improved with the use of anatomical priors, as illustrated in FIG. 9B as compared to FIG. 9A. When the anatomical labels are blurred with a 5 mm (FWHM) smoothing kernel to reflect the alignment uncertainty between the functional and anatomical images, as illustrated in FIG. 9C, the loss of lesion contrast compared to the aligned images illustrated in FIG. 9B is evident.

Detailed Description Text (31):

A wide range of applications of FDG PET for imaging cancer have been identified. The PET/CT scanner of the present invention is of particular utility in the thorax and abdomen due to the difficulty of aligning PET and CT images (with the exception of the brain) that are acquired on separate scanners, and because of the frequent difficulty of interpreting .sup.18 F-FDG PET studies in the abdomen. To date, over 65 cancer patients have been imaged on the PET/CT scanner according to the protocol described herein. Below are four illustrative case reports of lung cancer, lymphoma, pancreatic cancer and head and neck cancer. All PET images were corrected with CT-based attenuation correction, as described above, and reconstructed with FORE+OSEM, also as described above. In each case, PET imaging was performed sixty (60) minutes after an injection of 260 MBq of .sup.18 F-FDG. The PET scan duration varied depending on the study. The parameters for the spiral CT scans followed accepted protocols and were acquired with 10 mm sections, 200 mAs, 130 kV.sub.P and a pitch of 1.5. All CT scans presented herein were acquired without the administration of contrast agent.

<u>Detailed Description Text</u> (32):

A 72 year-old woman with primary squamous cell lung cancer was imaged on the PET/CT scanner. The PET emission scan was acquired for eight (8) minutes. The images shown in FIGS. 10A-C demonstrate a large lesion in the upper quadrant of the right lung. Although the lesion appears as a uniformly-attenuating, isodense mass on CT (FIG. 10A), the PET scan (FIG. 10B) reveals heterogeneous uptake consistent with a necrotic center and a rim of intense uptake representing high metabolic activity. The fused image (FIG. 10C) shows excellent alignment despite small differences due respiratory motion.

Detailed Description Text (33):

A 48 year-old woman with a history of non-Hodgkin's lymphoma was referred for a PET/CT scan. Spiral CT data were <u>acquired</u> over a limited whole-body range that extended from the upper part of the liver to the uterus. PET data were <u>acquired</u> at three contiguous_bed positions for a scan duration of thirteen (13) minutes at each hed position. An area of pronounced .sup.18 F-FDG uptake, located dorsally at the level of the lower abdomen, was seen on the PET images (FIG. 11B). Alignment with CT images demonstrated that the increased .sup.18 F-FDG uptake corresponded to a metastasis in the subcutaneous fat (FIG. 11C). The PET scan also demonstrated .sup.18 F-FDG accumulation in the pelvic region (not shown), distinct from normal bowel activity. The fused PET/CT image localized this focal .sup.18 F-FDG uptake to a known SI bone lesion seen on the CT. Due to the large cross-sectional area of the patient, there was significant CT beam hardening, as is apparent in the dorsal region in FIG. 11A.

Detailed Description Text (34):

A 38 year-old woman with confirmed pancreatic cancer was evaluated following placement of a biliary stent. An independently acquired contrast-enhanced CT scan revealed the presence of a large, 5 cm.times.3 cm, hypodense pancreatic mass. The PET scan was acquired for ten (10) minutes, and revealed a region of focally-increased uptake in the head of the pancreas (FIG. 12B) with an SUV of 5.3.

11 of 16 01/29/2003 9:41 AN The location of the impeased uptake was consistent with the hypodense mass seen on CT (FIG. 12C). In add on to the focal uptake in the creas, the whole-body PET/CT scan also revealed focally-increased .sup.18 F-FDG uptake in a right dorsal rib and in a mediastinal lymph node (not shown) suggesting spread of the disease.

Detailed Description Text (35):

Finally, a 72 year-old woman was referred for PET evaluation of a bulky supraglotic and hypopharangeal tumor, partially restricting the trachea, as illustrated in FIG. 13A. The PET scan was acquired for ten (10) minutes, and demonstrated intense uptake of FDG in the tumor with an SUV of over 30 (FIG. 13B). In addition, significant uptake was also seen in a soft tissue mass in the upper right neck and in a mass in the left neck adjacent to the jugular vein (not shown). The fused sagittal image of FIG. 13C, localizes the intense FDG uptake to the hypopharangeal mass.

Detailed Description Text (36):

The clinical studies illustrated in FIGS. 10-13 clearly illustrate the advantages and some of the challenges of the combined PET/CT scanner. A clinical analysis of the first 32 patients studied on the combined PET/CT has been completed and significant advantages of combined imaging are documented in distinguishing normal physiological uptake from possible malignancy, and in providing precise localization of lesions for subsequent surgical or biopsy procedures.

Detailed Description Text (37):

CT-based attenuation correction provides almost noiseless correction factors. However, a number of aspects have emerged in which CT-based attenuation correction requires significant improvement. These include accounting for the effects of respiratory motion, truncation of the CT field-of-view, beam hardening, and intravenous contrast agents. In the present invention, validation of the CT-based correction is performed by comparing emission scans reconstructed with CT-based factors to emission images reconstructed with factors obtained from standard PET transmission scans. For this purpose, the PET/CT scanner 10 is equipped with collimated cesium point sources operating in singles mode. Further improvement in SNR is also achieved by implementing continuous bed motion acquisition for the PET emission scan. Such an approach obviates the need to acquire overlapping bed positions that lead to axially varying SNR and lower overall efficiency. A feature of continuous bed motion is the use of list mode data acquisition, which also allows direct correction for patient movement during the scan.

Detailed Description Text (38):

The PET/CT scanner 10 is provided for the operation of a combined PET and CT scanner to perform anatomical (CT) and functional (PET) imaging in patients. The unique design is primarily targeted at whole-body oncology imaging in the thorax and abdomen with the conventional PET tracer 2-deoxy-2-(.sup.18 F)-fluoro-D-glucose (.sup.18 F-FDG). The combination of both functional and anatomical images, accurately aligned, obtained in a single scanner is a powerful diagnostic tool. All specific aims from the previous proposal have been achieved.

Detailed Description Text (39):

One stated object of the present invention is to generate attenuation correction factors for the PET data using the co-registered CT images. In the standard ECAT ART scanner, a transmission scan is performed using dual rotating .sup.68 Ge/.sup.68 Ga rod sources in coincidence mode or, more recently using .sup.137 Cs point sources with transmission data acquired in singles mode. A single photon emitter rather than a positron emitter can be used for transmission scanning because knowledge of the source position and the detection point of the transmitted photon on the opposing detector array provide the two points that are required to define a line-of-response. The detectors close to the point source are not used, and consequently the singles source can have higher activity than coincidence sources without creating a deadtime problem for the adjacent detectors. .sup.137 Cs with an emission energy of 662 keV and a half-life of 30 years has been used as a transmission source. The energy difference between 511 keV and 662 keV is corrected by scaling the measured attenuation factors. However, a recognized problem with singles transmission measurement is the high level of scatter in the transmission data, which can be limited in the case of coincidence imaging by the use of septa and rod windowing. To reduce scatter, the use of high activity collimated point sources has been implemented for transmission measurements on the ART. The collimators limit the acceptance of wide-angle scatters, similar to the septa shielding the detectors in a full-ring tomograph.

<u>Detailed Description Text</u> (40):

Compared to the rotating rod and point sources, CT-based attenuation correction has a number of important advantages. Namely, CT transmission scans that are <u>acquired</u> after the injection of the PET tracer will not be contaminated by 511 keV photons

emitted from the trace and the low detection ficiency of the CT detectors at 11 keV. Post-injection transmission scans are desirable in clinical settings as they increase both patient comfort and scanner throughput. Further, the CT data have much lower statistical noise than a standard PET transmission scan, thus reducing noise in the final attenuation-corrected PET emission image, that is especially important for whole-body PET imaging. In addition, the shorter times required for the collection of the CT transmission data allow longer times for the acquisition of the PET emission scan, thus lowering statistical noise even further for a given total scan duration. Still further, it is no longer essential to include standard PET transmission sources, thus eliminating the cost both of including these components and the periodic replacement of .sup.68 Ge/.sup.68 Ga rod sources. However, the prototype PET/CT scanner incorporates cesium sources to allow the PET and CT scanners to be operated independently. The availability of both the CT scanner and singles cesium sources also allows the CT-based attenuation correction algorithm to be compared directly with a standard PET attenuation correction based on a singles source transmission scan.

Detailed Description Text (41):

Although the combined scanner achieves the best possible overall coregistration between PET and CT, in regions such as the thorax, respiration and cardiac motion may result in some intrinsic misalignment. On the CT scan, lung boundaries and regions of either high or low attenuation are susceptible to motion artifacts. With the introduction of spiral CT, such as that used in the PET/CT scanner, motion artifacts are limited almost exclusively to the lingula and the lower lung segments in close contact with the left ventricle. The shorter scan times possible with spiral CT have essentially eliminated artifacts from cardiovascular motion. The spiral CT is acquired at breath hold, with the lungs inflated. The ungated PET image, on the other hand, represents an average over the scan duration of typically 5-10 minutes. During the scan, the patient breathes normally and the resulting PET image is an integration over the respiratory and cardiac cycles. The motion of the heart and chest wall results in reduced image spatial resolution. Exact CT and PET alignment of detailed structures in the anterior of the thorax is therefore not possible. It is important to avoid systematic effects. For example, the movement of the chest wall may be suppressed by breath holding during the CT scan, and hence there is a mismatch between the anterior wall position on CT and on PET. As a result of the movement of the chest wall, incorrect ACF's are generated by the algorithm, which could result in a reduction in .sup.18 F-FDG uptake in the anterior chest

Detailed Description Text (42):

CT scanners are designed with a transaxial field-of-view (FOV) of less than 50 cm diameter, a measure assuming the imaging of the thorax and abdomen is performed without the arms in the FOV. PET scanners for whole-body imaging typically have a transaxial FOV of 60 cm to allow the patient to be imaged with the arms in the FOV. This is because a whole-body PET scan may last 45-60 min, generally too long for a patient to remain comfortable with the arms above the head. The CT scan acquired with the arms in the field of view may therefore be truncated. This truncation results in artifacts at the edge of the field-of-view, and a small quantitative inaccuracy of about 10 HU maximum at the center of the field-of-view. The attenuation correction factors generated from the truncated CT image are therefore to some extent biased, affecting all. reconstructed pixel values.

Detailed Description Text (43):

The region truncated is generally across the arms. The average linear attenuation coefficient for the cross section of an arm, which is primarily composed of tissue and a small amount of bone, is used to fill in the boundaries as determined from a PET image reconstructed without attenuation correction, which is never truncated owing to the larger, 60 cm, FOV of the PET scanner. A good estimate of the outer skin surface is obtained from a FORE+OSEM reconstruction due to the statistical noise reduction outside the body surface (see FIGS. 7A,B). This estimate is made more robust, when necessary, by fitting a smooth 3D surface to the exterior of the skin layer as determined from the attenuated PET image. By comparing the outline of the body as determined from the CT and attenuated PET images, the missing volume is estimated. This volume is then added to the CT_image and set to the average linear attenuation coefficient for the arm.

Detailed Description Text (45):

It is known that image reconstruction with missing data of an arbitrary object is insoluble, but constraints on the image or sinogram data can make the problem more tractable. The missing region in the CT image is estimated by iterative reconstruction using the additional information described above to constrain the solution. Namely, the average value data (average attenuation for the arm), the

boundary data, and addional original line integral define non-truncated CT views are used for CT age reconstruction. This information is used with a variety of iterative image reconstruction methods that operate in either image space or sinogram space. In contrast to CT-based attenuation correction, the present invention uses the PET data for additional information when reconstructing the CT image.

Detailed Description Text (47):

Beam hardening results in a non-linear relationship between attenuation and the projection data. Such non-linearity requires an iterative approach to recover accurate attenuation values from projection data. A widely-used alternative method is to obtain suitable correction coefficients from look-up tables. Although in many imaging situations, beam hardening is satisfactorily corrected, for large patients the effect may be significant. The presence of arms in the FOV enhances the effect further, and standard beam hardening correction procedures are inadequate. The scaling of incorrect CT values to 511 keV results in biased attenuation correction factors that are then applied to the PET data. The effect is most problematic in the abdomen where maximum attenuation occurs.

Detailed Description Text (48):

The most widely-used study in .sup.18 F-FDG PET oncology is the whole-body scan. The patient is typically surveyed from head to upper thigh to identify localized regions of abnormal tracer uptake consistent with possible metastatic disease. To perform the scan, the patient bed is moved through the scanner in a sequence of discrete, overlapping steps. Data is acquired with the bed stationary, the PET scanner covering an axial extent of about 15 cm in each position. A total axial length of 80-100 cm is covered in 6-8 bed positions, with an overlap between bed positions varying from a few millimeters in 2D studies, up to 4 cm in 3D studies. The data for each bed position are acquired and reconstructed independently, and when all sets are complete, the data are assembled into a single whole body volume taking into account the overlap between each multi-bed position. Coronal and sagittal views and weighted projection images can be displayed in addition to the usual transverse sections.

Detailed Description Text (49):

The PET scanner used in the combined PET/CT device, the ECAT ART, acquires data fully in 3D. The axial sensitivity profile in three dimensions peaks in the center, resulting in highly non-uniform noise properties in the coronal and sagittal sections. To compensate for the non-uniform noise structure, a step of 12 cm is used with a 16 cm axial FOV, resulting in a 4 cm overlap at each end. In order to improve image quality in whole-body scans and to characterize the axial sampling schemes that lead to an optimal signal-to-noise (SNR) the bed is continually moved in an axial motion. The advantages of true continuous axial sampling include uniform axial SNR (except at the ends of the FOY), elimination of resolution artifacts due to axial undersampling, a reduction in the statistical noise contributed by the detector normalization factors, and a reduced sensitivity to small patient movements. Continuous axial sampling results in all detector rings acquiring data for every transaxial slice, eliminating normalization effects between detector rings. The continuously-acquired data is rebinned into finer axial sampling than the detector ring spacing, considerably reducing the aliasing artifacts due to axial undersampling arising with the multi-bed approach. The major advantage, especially for 3D data acquisition, is a more uniform SNR, eliminating the periodic variation in noise texture that may affect detectability. Continuous bed motion also results in more efficient use of the data because it avoids discarding the end planes of each bed position.

<u>Detailed Description Text</u> (50):

In order to implement finer axial sampling than the width of a detector ring with currently-available hardware, each LOR is acquired and stored separately in a list mode data stream and subsequently rebinned using a version of the FORE algorithm described above. A substantial increase in histogramming memory would be required to collect a full set of sinograms at finer axial sampling. The position of the bed at any moment can be read and integrated into the list mode data stream for use by the rebinning process. An additional advantage of list mode acquisition is that, if patient movement is monitored by an external device, motion correction can be applied directly to the individual LOR's in the list mode data stream. Uniform noise will reduce potential errors in the detection of small tumors, particularly when the tumor lies in an overlap region with high noise levels such as is encountered in the abdomen. Despite its desirable properties, continuous bed motion and monitoring of patient movement in whole-body scans has never been implemented for any PET scanner.

Detailed Description Text (51):

From the foregoing description, it will be recognized those skilled in the art that a combined PET at X-Ray CT tomograph offering and tages over the prior art has been provided. Specifically, the combined PET and X-Ray CT tomograph provides a tomograph for acquiring CT and PET images sequentially in a single device, overcoming alignment problems due to internal organ movement, variations in scanner bed profile, and positioning of the patient for the scan. An improvement to both the CT-based attenuation correction procedure and the uniformity of the noise structure in the PET emission scan is also provided. The PET/CT scanner includes an X-ray CT and two arrays of PET detectors mounted on a single support within the same gantry, and rotate the support to acquire a full projection data set for both imaging modalities. The tomograph acquires functional and anatomical images which are accurately co-registered, without the use of external markers or internal landmarks.

Detailed Description Paragraph Table (1):

Tube voltage [kV.sub.p]: 110, 130 Tube current [mA]: 63, 83, 105 Scan time per slice [s]: 1.3, 1.9 (multiple cycles possible) Slice thickness [mm]: 1, 2, 3, 5, 10 Gantry aperture [mm]: 600 Transaxial FOV [mm]: 450 Fan beam opening [deg]: 52.2

Detailed Description Paragraph Table (2):

CT value of air [HU] -1002 .+-. 10 CT value of water [HU] -2 .+-. 4 Cross-field uniformity [HU] <0.5 (with 20 cm water filled cylinder) Contrast scale (factory value) (1.90 .+-. 0.03) .multidot. 10.sup.-4 Contrast resolution (factory value) 2.5 mm/5 HU/1.9 s

Other Reference Publication (1):

A.C. Evans et al, "MRI-PET Correlation in Three Dimensions Using a <u>Volume-of-Interest (VOI)</u> Atlas," J Cereb Blood Flow Metab 11(2), A69-A78 (1991).

Other Reference Publication (5):

R.P. Woods et al, "MRI-PET registration with an automated algorithm," J Comp Assist Tomogr 17, 536-546 (1993).

Other Reference Publication (7):

R.L. Wahl et al, `Anatometabolic` tumor imaging: fusion of FDG PET with CT or MRI to localize foci of increased activity, J. Nucl. Med. 34, 1190-1197 (1993).

Other Reference Publication (26):

B. Bendriem et al., "A PET scatter correction using simultaneous <u>acquisitions</u> with low and high lower energy thresholds," IEEE 1993 Medical Imaging Conference Record 3, 1779-1783(1994).

Other Reference Publication (29):

X. Yan et al., "MAP estimation of PET images using prior anatomical information from MR scans," IEEE 1992 Medical Imaging Conference Record 2, 1201-1203 (1993).

CLAIMS:

1. A method for acquiring PET and CT images sequentially within a combined PET and X-Ray CT tomograph, the combined PET and X-Ray CT tomograph including a CT scanner having a patient gantry, a PET scanner having a patient gantry, a patient support for supporting a patient positioned within each said CT scanner patient gantry and said PET scanner patient gantry, and a display device, said method comprising the steps of: introducing a tracer into a patient for detection by said combined PET and X-Ray CT tomograph; waiting for an uptake period to expire, the tracer being circulated through and absorbed by the patient during said uptake period; placing the patient on said patient support; moving said patient support to position the patient within said CT scanner patient gantry such that a selected region to be studied is within a field of view of said CT scanner; acquiring a CT image of the selected region of the patient; correcting said CT image for artifacts due to field of view truncation, said step of correcting said CT image includes the steps of: obtaining a non-corrected PET image, said non-corrected PET image reconstructed without attenuation correction; determining a boundary of a truncated portion of the selected region of the patient using said non-corrected PET image; estimating a volume within said boundary of the truncated portion of the selected region using an average linear attenuation coefficient for the truncated portion of the selected region; and adding said volume to said CT image; reconstructing said CT image to achieve a reconstructed CT image; generating attenuation correction factors from said reconstructed CT image; moving said patient support to position the patient within said PET scanner patient gantry such that the selected region to be studied is within a field of view of said PET scanner; acquiring a PET image of the selected region of the patient; correcting said PET image for scatter to achieve a scatter-corrected PET image; applying said attenuation correction factors to said

15 of 16

scatter-corrected PET age to achieve an attenuation-crected PET image; and reconstructing said at huation-corrected PET image to lieve a reconstructed PET image.

- 6. The method of claim 1, during said step of acquiring a PET image of the selected region of the patient, further comprising the step of continuously moving said patient support in an axial direction within said patient gantry, whereby normalization effects between individual detector rings of said PET scanner are eliminated.
- 7. The method of claim 1 wherein said CT scanner patient gantry is separate from and fixed relative to said PET scanner patient gantry, said patient support being movable between said CT scanner patient gantry and said PET scanner patient gantry, whereby said step of acquiring a CT image of the selected region of the patient is accomplished within said CT scanner patient gantry, and whereby said step of acquiring a PET image of the selected region of the patient is accomplished within said PET scanner patient gantry.
- 8. The method of claim 1 wherein said CT scanner patient gantry is separate from said PET scanner patient gantry, wherein at least one of said CT scanner and said PET scanner is movable with respect the other, and wherein said patient support is movable between said CT scanner patient gantry and said PET scanner patient gantry, whereby said step of acquiring a CT image of the selected region of the patient is accomplished within said CT scanner patient gantry, and whereby said step of acquiring a PET image of the selected region of the patient is accomplished within said PET scanner patient gantry.
- 9. The method of claim 8 wherein said step of <u>moving said patient support</u> to position the <u>patient</u> within said CT scanner <u>patient gantry</u> is accomplished by <u>moving said CT scanner</u> to receive said <u>patient bed</u> within said CT scanner <u>patient gantry</u>.
- 10. The method of claim 8 wherein said step of moving said patient support to position the patient within said PET scanner patient gantry is accomplished by moving said PET scanner to receive said patient bed within said PET scanner patient gantry.
- 11. A method for acquiring PET and CT images sequentially within a combined PET and X-Ray CT tomograph, the combined PET and X-Ray CT tomograph including a patient gantry for use with both a CT scanner and a PET scanner, a patient support for supporting a patient positioned within said patient gantry, and a display device, said method comprising the steps of: introducing a tracer into a patient for detection by said combined PET and X-Ray CT tomograph; waiting for an uptake period to expire, the tracer being circulated through and absorbed by the patient during said uptake period; placing the patient on said patient support; moving said patient support to position the patient within said patient gantry such that a selected region to be studied is within a field of view of said CT scanner; acquiring a CT image of the selected region of the patient; correcting said CT image for artifacts due to field of view truncation, said step of correcting said CT image includes the steps of: obtaining a non-corrected PET image, said non-corrected PET image reconstructed without attenuation correction; determining a boundary of a truncated portion of the selected region of the patient using said non-corrected PET image; estimating a volume within said boundary of the truncated portion of the selected region using an average linear attenuation coefficient for the truncated portion of the selected region; and adding said volume to said CT_image; reconstructing said CT image to achieve a reconstructed CT image; generating attenuation correction factors from said reconstructed CT image; moving said patient support to position the patient within said patient gantry such that the selected region to be studied is within a field of view of said PET scanner; acquiring a PET image of the selected region of the patient; correcting said PET image for scatter to achieve a scatter-corrected PET image; applying said attenuation correction factors to said scatter-corrected PET image to achieve an attenuation-corrected PET image; and reconstructing said attenuation-corrected PET image to achieve a reconstructed PET image.
- 16. The method of claim 11, during said step of acquiring a PET image of the selected region of the patient, further comprising the step of continuously moving said patient support in an axial direction within said patient gantry, whereby normalization effects between individual detector rings of said PET scanner are eliminated.

Generate Collection Print

L22: Entry 8 of 14

File: USPT

Aug 14, 2001

DOCUMENT-IDENTIFIER: US 6275721 B1

TITLE: Interactive MRI scan control using an in-bore scan control device

Abstract Text (1):

A scan control device located in the bore of an MRI system magnet includes tracking coils and a display. Location and alignment of the scan control device is tracked by the MRI system using signals acquired from the tracking coils. These signals are also used to update the scan parameters such that the scan plane of the image acquired by the MRI system is controlled by the scan control device location and orientation. The image is produced on the display to provide an attending physician with interactive control of the image from the magnet bore.

Brief Summary Text (2):

The field of this invention is <u>magnetic resonance</u> imaging (MRI) methods and systems. More particularly, the invention relates to interactive control of the scan plane prescription during an MRI guided procedure.

Brief Summary Text (3):

When a substance such as human tissue is subjected to a uniform magnetic field (polarizing field B.sub.0) in the z_direction of a Cartesian coordinate system, the individual magnetic moments of the nuclear spins in the tissue attempt to align with this polarizing field, but precess about the field in random order at their characteristic Larmor_frequency. If the substance, or tissue, is also subjected to a magnetic field (excitation field B.sub.1) which is in the x-y plane and which is near the Larmor frequency, the net aligned moment M.sub.z may be rotated, or "tipped", into the x-y plane to produce a net transverse magnetic moment M.sub.t. A signal is emitted by the excited spins after the excitation signal B.sub.1 is terminated, and this signal may be received and processed to form an image.

Brief Summary Text (4):

When utilizing these signals to produce images, magnetic field gradients (G.sub.x, G.sub.y and G.sub.z) are employed. Typically, the <u>region to be imaged</u> is scanned by a sequence of measurement cycles, or "views", in which these gradients vary according to the particular localization method being used. The resulting set of received nuclear <u>magnetic resonance (NMR)</u> signals are digitized and processed to reconstruct the image using one of many well known reconstruction techniques.

Brief Summary Text (5):

Intra-operative MR imaging is employed during a medical procedure to assist the physician in guiding an instrument. For example, during a needle biopsy the MRI system is operated in a real-time mode in which image frames are produced at a high rate so that the physician can monitor the location of the needle as it is inserted. A locator device such as that described in Dumoulin et al. U.S. Pat. No. 5,271,400 issued Dec. 21, 1993 and U.S. Pat. No. 5,307,808, issued May 3, 1994, both of which are assigned to the instant assignee, may be used to track the location of the instrument and provide coordinate values to the MRI system which enable it to mark the location of the instrument in each reconstructed image. The medical instrument is attached to a handpiece that is manipulated by the physician and whose position is detected by surrounding sensors. For example, the handpiece may emit light from two or more light emitting diodes which is sensed by three stationary cameras.

Brief Summary Text (6):

Tracking devices which employ the MRI system to locate markers in the medical device have also been developed. As described in Dumoulin et al. U.S. Pat. Nos. 5,271,400, 5,307,808 and 5,318,025, Souza et al. U.S. Pat. No. 5,353,795 and Watkins et al. U.S. Pat. No. 5,715,822, each of which is assigned to the instant assignee, such tracking systems employ a small coil attached to a catheter or other medical device to be tracked. A NMR pulse sequence is performed to establish desired magnetic field gradients to produce transverse magnetization at the location of the tracking coil

carried by the tracked evice. The location of the tracing coil is determined and is superimposed at the orresponding location in a media limage acquired with the same MRI system.

Brief Summary Text (7):

During an interactive MRI diagnostic procedure or interventional procedure, it is common for the operator to frequently change the scan plane coordinates and orientation. It may also be desirable for the operator to modify the imaging pulse sequence parameters or exercise other control over the MR scanner in a rapid fashion, especially for interactive control of real-time imaging sequences. Additionally, it may be desirable for the operator to view in-bore the results of image formation on a screen built into the controlling device. There is currently no method that permits an operator working in-bore to perform such operations.

Brief Summary Text (9):

A scan control device for use in the bore of an MRI system to interactively control the scan plane prescription includes a housing that encloses a plurality of tracking RF coils and a corresponding plurality of MR signal sources. The MRI system periodically performs tracking coil NMR pulse sequences during the MRI interactive procedure that acquire tracking coil data from which the position and orientation of the scan control device are determined and then used to update the scan plane prescription of the NMR imaging pulse sequence being performed. During the MRI interactive procedure, the operator manipulates the scan control device to point at particular anatomy of interest and indicate the desired viewing orientation. The tracking coil NMR pulse sequences are interleaved with the imaging NMR pulse sequences, and the acquired tracking coil data are used to calculate scan plane parameters for updating the NMR pulse sequence parameters.

Brief Summary Text (10):

Another aspect of the invention is the provision of visual feedback to the operator during the MRI interactive procedure. The scan control device may also house a display which produces the image reconstructed from data acquired with the NMR imaging pulse sequences. As the scan control device is manipulated about the patient, the NMR imaging pulse sequence is continuously updated and the reconstructed image on the display is updated to promptly indicate to the operator the imaged anatomy.

Brief Summary Text (11):

Yet another aspect of the invention provides the operator with the ability to alter the scan prescription during the MRI interactive procedure. The scan control device may include manually operable data input devices that can be used by the operator to alter the NMR imaging pulse sequence prescription. For example, parameters such as transmit-receive (TR) period, excitation pulse flip-angle or field of view may be adjusted by the operator while in the bore of the MRI system magnet.

<u>Drawing Description Text</u> (2):

FIG. 1 is a block diagram of an_MRI system employing the invention;

Drawing Description Text (3):

FIG. 2 is a schematic diagram of a <u>tracking</u> coil and associated MR signal source used to practice the invention;

Drawing Description Text (4):

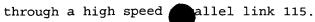
FIGS. 3 is a pictorial view of a scan control device which employs three of the tracking coils shown in FIG. 2;

<u>Drawing Description Text</u> (5):

FIG. 4 is a graphic representation of an NMR pulse sequence used by the MRI system of FIG. 1 to measure the position of the tracking coil of FIG. 2; and

<u>Detailed Description Text</u> (2):

FIG. 1 illustrates the major components of an MRI system which incorporates the invention. A magnet system 103 produces a polarizing magnetic field in a region commonly referred to as the magnet "bore". Operation of the system is controlled from an operator console 100 which includes a keyboard and control panel 102 and a display 104. Console 100 communicates through a link 116 with a separate computer system 107 that enables an operator to control the production and display of images on the screen of display 104. Computer system 107 includes a number of modules which communicate with each other through a backplane 105. These include an image processor module 106, a CPU (central processing unit) module 108, and a memory module 113 known in the art as a frame buffer for storing image data arrays. Computer system 107 is linked to a disk storage 111 and a tape drive 112 for storage of image data and programs, and communicates with a separate system control 122



Detailed Description Text (3):

System control 122 includes a set of modules connected together by a backplane 118 These include a CPU module 119 and a pulse generator module 121 which is coupled to operator console 100 through a serial link 125. System control 122 receives commands from the system operator through link 125 which indicate the scan sequence to be performed. Pulse generator module 121 operates the system components in accordance with a set of scan parameters to carry out the desired scan sequence, producing data that indicate the timing, strength and shape of the RF (radio frequency) pulses to be produced, and the timing and length of the data acquisition window. Pulse generator module 121 is coupled to a set of gradient amplifiers 127 to control the timing and shape of the gradient pulses to be produced during the scan. Pulse generator module 121 also receives patient data from a physiological acquisition controller 129 that receives signals from a number of different sensors attached to the patient, such as ECG (electrocardiogram) signals from electrodes or respiratory signals from a bellows. Pulse generator module 121 is also coupled to a locator system 133 that interfaces with a scan control device 132. As described in more detail below, locator system 133 performs a number of functions including: monitoring location and orientation of scan control device 132; calculating updated scan parameters for pulse generator 121; and supplying image data to a display 134 on scan control device 132.

Detailed Description Text (4):

The gradient waveforms produced by pulse generator module 121 are applied to a gradient amplifier system 127 comprised of G.sub.x, G.sub.y and G.sub.z amplifiers. Each gradient amplifier excites a corresponding gradient coil in magnet system 103 to produce the magnetic field gradients used for position encoding acquired signals. A transceiver module 150 in system control 122 produces pulses which are amplified by an RF amplifier 151 and supplied to an RF coil magnet system 103 by a transmit/receive switch 154. The resulting signals radiated by the excited nuclei in the patient may be sensed by the same RF coil and supplied through transmit/receive switch 154 to a preamplifier 153. The amplified NMR signals are demodulated, filtered, and digitized in the receiver section (not shown) of transceiver 150. Transmit/receive switch 154 is controlled by a signal from pulse generator module 121 to electrically connect RF amplifier 151 to the RF coil during the transmit mode and to connect the RF coil to preamplifier 153 during the receive mode. Scan control device 132 includes three RF tracking coils which acquire NMR signals that indicate the location and orientation of the scan control device. These NMR signals are provided to a set of three pre-amplifiers 152 which apply the amplified signals to transceiver module 150.

<u>Detailed Description Text</u> (5):

The NMR signals picked up by an RF coil in magnet assembly 103 are digitized by transceiver module 150 and transferred to a memory module 160 in system control 122. When an array of k-space data (i.e., spatial frequency space data) has been acquired in memory module 160, an array processor 161 operates to Fourier transform the k-space data into an array of image data which is presented to the attending physician on a display 134 that forms part of scan control device 132. This image data may also be conveyed through parallel link 115 to computer system 107 where it is stored in disk memory 111. In response to commands received from operator console 100, the image data may be archived on tape drive 112, or may be further processed by image processor 106 and conveyed to operator console 100 and presented on display

Detailed Description Text (6):

Data acquired from the tracking RF coils in scan control device 132 are reconstructed into profiles for use by locator system 133 to determine location of the desired scan plane. Locator system 133 employs this information to alter the scan parameters used by pulse generator module 121 to acquire subsequent image data.

Detailed Description Text (7):

While a conventional MRI system may be used to implement the invention, in the preferred embodiment an MRI system which is designed to allow access by a physician is employed. When an intra-operative MR imaging procedure is conducted, a patient is placed in the bore of magnet system 103 and a region of interest in the patient is aligned near the system isocenter located between two, spaced magnet rings 140 and 142. A physician standing between magnet rings 140 and 142 has unrestricted access to the region of interest in the patient, and scan control device 132 may be moved around within the magnet bore to point at specific anatomy.

Detailed Description Text (8):

The images to be produced by the MRI system are prescribed by selecting an appropriate NMR imaginary pulse sequence to be executed pulse generator 121. Location and orientation of the slices or 3D region to be imaged are also prescribed and are determined by the particular patient anatomy that the physician wants to see during the procedure being performed. This image is produced on display 134 which is a part of scan control device 132 that is in the bore of magnet system 103 with the patient and physician. Scan control device 132 may be manipulated by the physician to "point" at specific patient anatomy and this "pointing" is sensed by the tracking coils and used to update the scan parameters. As a result, an updated image is acquired, reconstructed and produced on display 134 which depicts the anatomy of interest to the physician. The physician can thus move scan control device 132 over and around the patient and the MRI system continuously updates the image on display 134 to depict the anatomy of interest.

Detailed Description Text (10):

Housing 175 is substantially rectangular in shape and includes a pair of handles 177 mounted on each of its sides. The attending physician may hold scan control device 132 by handles 177 and "aim" it at the patient. Three tracking coils 200 are mounted within housing 175 and connected through cable 179 to pre-amplifiers 152 (FIG. 1). Tracking coils 200 define a plane, and an imaginary line between the top two tracking coils 200 defines an orientation in that plane.

<u>Detailed Description Text (11):</u>

Scan control device 132 includes a set of thumb switches 180 mounted inboard of each handle 177. The thumb switches can be toggled by the physician to increase or decrease the value of a scan parameter to enable the image produced on display 134 to be changed during the procedure. The particular scan parameters that may be adjusted by thumb switches 180 is configurable by the operator; however, a predetermined one of the thumb switches is always configured to adjust the distance of an image plane 182 from the plane of scan control device 132 along a sighting axis 184. The sighting axis extends from the center of the display, perpendicular to the plane defined by the three tracking coils 200. Image plane 182 is centered on axis 184 at a distance that is manually adjustable with thumb switch 180. The physician can thus aim scan control device 132 at the patient from any desired angle and orientation and adjust the predetermined one of thumb switches 180 to move scan plane 182 to the proper depth.

<u>Detailed Description Text</u> (12):

A second one of thumb switches 180 may be set in one position to continuously update the location and orientation of scan plane 182 as scan control device 132 is moved around within the bore of the magnet. When the desired image is obtained, this second one of the thumb switches may be toggled to a second position which locks scan plane 182 in a fixed orientation and position. The physician may then operate the other configured thumb switches 180 to adjust such scan parameters as field of view. TR and flip-angle until the best image is obtained for the particular medical procedure being performed. Other parameters, such as window width and level used during image display may also be adjusted.

Detailed Description Text (13):

Scan control device 132 is connected to locator system 133 (FIG. 1) by a cable 186 which conveys video data to display 134 and conveys signals from thumb switches 180 back to locator system 133. Scan control device 132 is constructed of materials compatible with the environment in the bore of an MRI system, and suitable filtering and shielding of electrical signals is performed, as is known in the art.

Detailed Description Text (14):

FIG. 2 shows one of the three small RF tracking coils 200 that are enclosed in scan control device 132 (FIG. 3). Each of these RF tracking coils contains as a sample 202 a spherical glass container (with a 5 millimeter internal diameter) of water doped with CuSO.sub.4 to provide a "spin--spin" or transverse relaxation time T.sub.2 of approximately 10 milliseconds. Each sample 202 is enclosed in a tightly fitting spherically wound RF coil 200 tuned to 63.9 MHz (for 1.5 Tesla .sup.1 H NMR). RF coils 200 are receive coils and include a switchable PIN diode 204 for decoupling during RF transmission by the MRI system RF body coil.

Detailed Description Text (15):

The position of a tracking coil 200 relative to the gradient isocenter is measured using the position measurement NMR pulse sequence shown in FIG. 4. This gradient recalled echo pulse sequence yields a signal that is essentially a Fourier transform of a projection of the coil location along the readout gradient direction. Assuming that tracking coil 200 is small, its position S.sub.1 is modeled by: ##EQU1##

Detailed Description Text (16):

where .omega. is the surement angular frequency of gradient echo signal relative to .omega..s 0, the Larmor frequency, and 6 b.1 is the applied readout gradient. The three-dimensional position of each tracking coil 200 can be identified from three linearly independent gradient echoes.

Detailed Description Text (17):

As described in the above cited Souza et al. U.S. Pat. No. 5,353,795, issued Oct. 11, 1994 and entitled "Tracking System To Monitor The Position Of A Device Using Multiplexed Magnetic Resonance Detection", which is incorporated herein by reference, errors arising from resonance offset conditions make it necessary to acquire more than three tracking coil measurements. While it is possible to acquire two measurements along each gradient axis to obtain the necessary error free tracking NMR data, such an approach requires six separate measurements. In a preferred embodiment, a Hadamard MR tracking sequence is performed using the measurement pulse sequence of FIG. 4. This tracking sequence requires only four separate measurements to acquire a complete NMR tracking coil data set.

Detailed Description Text (18):

As shown in FIG. 4, the tracking coil measurement pulse sequence includes a non-selective RF excitation pulse 250 which is applied to the MRI system whole body RF coil in magnet system 103 (FIG. 1). Pulse 250 has a flip angle of from 10 to 60 degrees and produces transverse magnetization in spins located throughout the magnet bore. Three gradient waveforms 256, 257 and 258 are then applied to respective gradient coils in magnet system 103 (FIG. 1) to produce a gradient recalled NMR echo signal. The NMR signals acquired by each RF tracking coil are provided separately to transceiver module 150 (FIG. 1). The three gradient waveforms 256, 257 and 258 are applied along the respective G.sub.x, G.sub.y and G.sub.z gradient axes in the magnet system and each of the waveforms includes a respective dephase lobe 260, 261 and 262 and a respective readout lobe 264, 265 and 266. The area of each dephasing lobe 260-262 is equal to one-half the area of respective readout lobes 264-266.

Detailed Description Text (19):

In the measurement pulse sequence of FIG. 4, all of the gradients 256-258 have the same polarity, herein designated "-". This data acquisition pulse sequence is performed a total of four times with the polarity of the G.sub.x, G.sub.y and G.sub.z gradient pulses selectively reversed as set forth in Table 1.

Detailed Description Text (20):

As indicated above, four NMR tracking signals 254 from each tracking coil 200 (FIG. 3) are Fourier transformed to produce four corresponding projections P.sub.1, P.sub.2, P.sub.3 and P.sub.4. Together, these four projections form an NMR tracking data set from which the x, y and z coordinates of the tracking coil position can be calculated.

Detailed Description Text (21):

The scan is carried out by a series of steps depicted in FIG. 5. When the procedure is started, the operator enters the initial scan prescription as indicated at step 270. This step includes the selection of an appropriate NMR imaging pulse sequence and the particular scan parameters that locate and orient the slice plane or 3D volume which is to be imaged.

<u>Detailed Description Text</u> (22):

At the next step 272, the present positions of tracking coils 200 are measured. This is done by acquiring the four projections P.sub.1 -P.sub.4 as described above with the Hadamard encoding indicated in Table 1. The locations of the signal peaks are then combined as follows:

<u>Detailed Description Text</u> (23):

to provide the coordinates S.sub.x, S.sub.y and S.sub.z of tracking coil 200.

Detailed Description Text (24):

A loop is next entered in which image data and tracking coil data are acquired in an interleaved manner and the displayed image is updated on a real-time basis. As indicated at step 274, scan parameters for pulse generator 121 (FIG. 1) are updated using the tracking coil position data as well as any changes in the scanning parameters suplied by the operator from thumb switches 180 (FIG. 3).

Detailed Description Text (25):

As indicated above with reference to FIG. 3, the positions of the three tracking coils 200 define the location and orientation of the plane of display 134. The desired imaging plane 182 is offset from this display plane along sighting axis 184 by an amount determined by operation of a thumb switch 180. This updated information is used to calculate the appropriate rotation matrices required to produce oblique

MR images. This update information is also used to procee the appropriate frequency and phase of ets required to position imaginaplane 182 with respect to the MRI system isocenter. Any other changes in scan parameters supplied from thumb switches 180 are also updated and applied to pulse generator 121 (FIG. 1).

Detailed Description Text (26):

After the scan parameters are updated, image data are <u>acquired</u> at step 276, using the updated scan parameters. Depending on the particular image pulse sequence being used, data for an entire image reconstruction may be <u>acquired</u>, or data for only part of the k-space image data may be <u>acquired</u>. In either instance, the <u>acquired</u> image data are used to reconstruct an updated image, as indicated at step 278, and this updated image is supplied to display 134 on scan control device 132 (FIG. 1).

Detailed Description Text (28):

If the interactive procedure has finished, as determined at step 280, the process ends. Otherwise, the process loops back to enter scan prescription changes at step 282 and to measure the tracking coil position at step 284. The scan prescription changes are entered from scan control device 132 and the tracking coil positions are updated by performing the position measurement NMR pulse sequence of FIG. 4. Four measurement pulse sequences may be performed as described above to provide four updated projections P.sub.1 -P.sub.4 for each of the three tracking coils 200. In the alternative, only one projection may be updated as described in co-pending Dumoulin et al. U.S. patent application Ser. No. 09/199,405, filed Nov. 25, 1998, assigned to the instant assignee, and entitled "High Speed Tracking of Interventional Devices Using an MRI System", which is incorporated herein by reference. The process then returns to steps 274-279 to update the scan parameters and acquire an updated image as described above.

Detailed Description Text (29):

It should be apparent that many variations are possible from the preferred embodiment described above. For example, rather than continuously updating image on display 134 as scan control device 132 is moved about the patient, a trigger may be provided which must be operated by the physician before an updated image is acquired. This will enable scan control device 132 to be moved without changing the displayed image. When scan control device 132 is properly aligned, the physician may then operate the trigger and acquire an updated image which is reconstructed and displayed. It is also possible to use two different imaging pulse sequences during the procedure. A first pulse sequence may be used during normal interactive display of images as scan control device 132 is moved. Such pulse sequences may provide very fast acquisition, but not produce optimal diagnostic images. When device 132 is in position, however, the physician can operate the trigger and acquire a high resolution image using a different pulse sequence. The physician can thus manipulate scan control device 132 into the desired orientation using the real-time images produced on display 134 for guidance, and then produce a high resolution, clinical image on display 134.

Detailed Description Text (30):

It is also possible to locate the position and orientation of scan control device 132 using other methods. For example, three light sources can be mounted on housing 175 (FIG. 3) and their positions within the bore of the MRI system monitored by cameras

Detailed Description Text (31):

As another variation, a marker in the form of an MR active substance may be imbedded in scan control device 132. The marker has a unique shape which can be easily identified when scan control device 132 is in the <u>field of view of the acquired</u> image. For example, three of spherical glass samples 202, described above in conjunction with FIG. 3, may be positioned close together in the reconstructed image.

Detailed Description Text (32):

Scan control device 132 may also be used to guide the medical procedure. In one embodiment, for example, a laser diode is mounted on the back of housing 175 (FIG. 3) and directs a visible laser beam along sighting axis 184. A visible spot is produced on the patient where sighting axis 184 impinges, and this spot can serve as a locating guide for a biopsy needle or the like. Scan control device 132 can also serve to orient the medical device. In this instance, a mechanical guide (not shown) is mounted to the back of housing 175 for holding the medical instrument (e.g. biopsy needle) along sighting axis 184. The medical instrument may thus be positioned and oriented at an angle that will operate on the particular anatomy indicated by a marker in the reconstructed image on display 134. This provides real-time feedback to the physician to monitor and adjust patient therapy. If the resulting system is awkward to manually position with accuracy, it is also possible

to mount control device 132 on an articulated arm (not pown). A joystick is used to operate the articulated arm to move scan control device 32 into proper position and orientation as determined by the real-time images produced on display 134.

Detailed Description Paragraph Table (1):
TABLE 1 G.sub.x G.sub.y G.sub.z acquisition 1 - - acquisition 2 + + - acquisition 3 + - + acquisition 4 - + +

CLAIMS:

- 1. An MRI system comprising:
- a magnet system for producing a polarizing magnetic field in a magnet bore;
- a scan control device including a display mounted therein, the scan control device being moveable within the magnet bore and being manipulatable to aim at a subject when said subject is located in the magnet bore;
- a set of tracking coils mounted to the scan control device;
- a pulse generator for controlling operation of the MRI system to perform an imaging pulse sequence in accordance with a set of scan parameters and for controlling operation of the MRI system to acquire NMR tracking signals from the set of tracking coils;
- a locator system for calculating location and orientation of the scan control device from the <u>acquired NMR tracking</u> signals and producing updated scan parameters for the pulse generator; and

image reconstruction means for receiving NMR imaging signals produced by the imaging
pulse sequence and reconstructing an image of the subject;

wherein the location of the image is determined by the updated scan parameters produced by the locator system.

- 2. The MRI system as recited in claim 1 in which the display produces the image thereon.
- 3. The MRI system as recited in claim 1 wherein the set of <u>tracking</u> coils comprises three <u>tracking</u> coils.
- 4. The MRI system as recited in claim 1 in which the scan control device includes a manually operable input device for changing a selected one of the scan parameters.
- 5. The MRI system as recited in claim 1 in which the scan control device includes a housing which can be hand-held and hand-aimed.
- 6. The MRI system as recited in claim 5 in which a pair of handles are mounted to opposite sides of the housing and the display is mounted between the handles.
- 7. The MRI system as recited in claim 5 in which a manually operable input device is mounted to the housing and is manually operable to change a selected one of the scan parameters.
- 8. The MRI system as recited in claim 1 wherein the image reconstruction means comprises a transceiver, a memory module coupled to said transceiver, and an array processor responsive to said memory module for providing data for reconstructing said image of the subject.
- 9. A method for performing an MRI scan with an MRI system having a magnet system for producing a polarizing magnetic field in a magnet bore, comprising the steps of:
- a) performing an imaging pulse sequence in accordance with a set of scan parameters to acquire NMR imaging data;
- b) reconstructing an image using the acquired imaging data;
- c) displaying the image on a display mounted on a scan control device;
- d) changing a selected scan parameter using the scan control device;
- e) updating the imaging pulse sequence; and,

7 of 8 01/29/2003 9:34 At

- f) repeating steps a b), c) and d).
 - 12. The method as recited in claim 11 including the additional step of determining the scan control device location by acquiring NMR data with the MRI system from tracking coils mounted to the scan control device.
 - 13. The method as recited in claim 12 including the step of interleaving the acquired tracking coil NMR data with the acquired NMR imaging data.
 - 20. A method for performing an MRI scan of a subject with an MRI system having a magnet system for producing a polarizing magnetic field in a magnet bore, comprising the steps of:
 - a) performing an imaging pulse sequence in accordance with a set of scan parameters to acquire NMR imaging data;
 - b) reconstructing an image using the acquired imaging data;
 - c) displaying the image on a display mounted on a moveable hand-held scan control device;
 - d) moving the scan control device relative to the <u>subject</u> and within the magnet bore; and,
 - e) updating the image on the display responsive to the moving step.